Finite element model for free vibration analysis of functionally graded doubly curved shallow shells by using an improved first-order shear deformation theory

Finite element model for free vibration analysis of functionally graded doubly curved shallow shells by using an improved first-order shear deformation theory

Soufiane Benounas[1], Mohamed-Ouejdi Belarbi[**1,2], Pham Van Vinh[3,4], Ahmed Amine Daikh[5,6], Nicholas Fantuzzi[7]

[1]*Laboratoire de Recherche en Génie Civil, LRGC, Université de Biskra, B.P. 145, R.P. 07000, Biskra, Algeria*
[2]*Department of Civil Engineering, Lebanese American University, Byblos, Lebanon*
[3] *Institute of Physics and Mechanics, Peter the Great St. Petersburg Polytechnic University, Saint Petersburg, Russia*
[4]*Department of Solid Mechanics, Le Quy Don Technical University, Hanoi, Vietnam*
[5] *Artificial Intelligence Laboratory for Mechanical and Civil Structures, and Soil, University Centre of Naama, Naama, Algeria*
[6] *Laboratoire d'Etude des Structures et de Mécanique des Matériaux, Département de Génie Civil, Faculté des Sciences et de la Technologie, Université Mustapha Stambouli B.P. 305, Mascara*
[7]*University of Bologna, Viale del Risorgimento 2, Bologna, 40136, Italy*

Abstract.

A novel finite element model based on the improved first-order shear deformation theory (IFSDT) is proposed to investigate the vibration behavior of functionally graded doubly curved shallow shells in this study. The IFSDT adopted in the present model eliminates the need for a shear correction factor by making a simplified assumption about the transverse shear stress. This assumption ensures that the model accurately predicts both normal and shear stresses across the shell's thickness while satisfying the free traction conditions on the shell's upper and lower surfaces. Five types of doubly curved shells, named flat plates, spherical shells, hyperbolic parabolic shells, cylindrical shells, and elliptical paraboloid shells, are selected here for numerical analysis. The fundamental equations are derived from the Hamiltonian principle, and they are solved numerically by the finite element method. The accuracy and efficiency of the proposed finite element model are demonstrated via several comparison studies. A comprehensive parameter study is then presented to illustrate the influence of some parameters on the vibration behaviors of the functionally graded doubly curved shallow shells. The outcomes of this research provide a robust benchmark for the design, testing, and manufacture of doubly curved shallow shells and will inform future investigations into shell structures.

Keywords: Functionally graded, Vibration, Finite element method, Doubly curved shells, Shear deformation theory

* Corresponding author: Professor (Mohamed-Ouejdi Belarbi): Email address: mo.belarbi@univ-biskra.dz

1. Introduction:

Advanced composites represent a cutting-edge class of materials that have revolutionized various industries by combining the unique properties of different components to create materials with superior performance characteristics [1]. Among these advanced composites, functionally graded materials (FGMs) stand out as a particularly innovative and versatile subset. FGMs represent a departure from traditional homogeneous materials by seamlessly blending two or more distinct materials with varying compositions and properties across a designated spatial gradient [2-6]. This strategic design enables FGMs to deliver tailored and highly specialized performance, making them a topic of great interest in materials science and engineering.

The plates and shells represent significant and widespread structures across various practical engineering and industrial fields [7-10]. As a result, gaining a comprehensive understanding of the mechanical behavior of these structures poses a major challenge for researchers. Punera and Kant [11] carried out a critical review of stress and vibration analyses of FG shell structures. To explore these structures, researchers employ different shear deformation theories, such as classical theory (CPT), first-order shear deformation theory (FSDT), higher-order shear deformation theories (HSDTs), and quasi-3D shear and normal deformation theories. Additionally, both analytical and numerical solutions are utilized to address the governing equations of motion for these structures.

The vibrational behaviour of FG structures is important across numerous engineering and scientific disciplines due to its profound impact on the functionality, safety, and longevity of various systems. Loy et al. [12] conducted a study on the vibration characteristics of cylindrical shells constructed from an FG comprising stainless steel and nickel. Kim [13] concentrated on investigating the vibration properties of FGM plates with initial stress. The displacement elements were expressed through the Fourier series, and the frequency equation was obtained through the Rayleigh–Ritz method. Ferreira et al. [14] used the global collocation method with multiquadric radial basis functions in their analyses of the free vibration characteristics of FG plates. Belarbi et al. [15] analysed the nonlocal vibration response of FG nanoplates using a layerwise finite element formulation. Matsunaga [16] employed the method of power series expansion to explore the free vibration and stability characteristics of FG circular cylindrical shells. Zhao and co-authors [17] employed the mesh-free kp-Ritz method to analyse the free vibration behaviour of FG plates. Pradyumna and Bandyopadhyay [18] introduced the fundamental frequencies and critical buckling load for different types of FGM shells, employing a higher-order shear deformation theory. Malekzadeh and Beni [19] employed the differential quadrature method (DQM) along with the geometric mapping technique to investigate the free vibration of FG arbitrary straight-sided quadrilateral plates under thermal conditions. Talha and co-authors [20] applied the HSDT to investigate both the static and dynamic behaviours of FG plates under various boundary conditions. Kiani and his colleagues [21] explored the thermoelastic free vibration and dynamic behaviour of a functionally graded material doubly curved panel using an analytical hybrid Laplace–Fourier transformation. Kim [22] examined,

through an FSDT, the free vibration response of FG cylindrical shells supported by an elastic foundation modeled using the Pasternak model. Fallah et al. [23] extended the Kantorovich method to investigate the free vibration of moderately thick FG plates. Natarajan and their colleagues [24] introduced an eight-node quadrilateral element based on the HSDT for the analysis of FG plates. Viola et al. [25] introduced a 2D unconstrained third order shear deformation theory (UTSDT) for the moderately thick FG cylindrical shells subjected to mechanical loads. Based on a HSDT, Neves et al. [26] investigated the free vibration phenomena of FG shells using radial functions collocation method. Jha et al. [27] conducted an analysis of the stress and free vibrations of FG plates under severe thermo-mechanical loading, employing an HSDT. Kar and Panda [28] conducted an analysis of the free vibration behavior of functionally graded (FG) spherical shell panels using a nine-nodded quadrilateral element based on a HSDT.

Tornabene et al. [29] examined the free vibration characteristics of doubly curved FG shells. Their approach involved utilizing equivalent single-layer (ESL) theories derived from the Carrera unified formulation (CUF) with consideration of the zig-zag effect. Later, Huy Bich et al. [30] investigated the nonlinear dynamic behavior and nonlinear vibrations of FGM shells using a combination of FSDT, smeared stiffeners Lekhnitsky's technique, and stress function. Bahadori and Najafizadeh [31] employed an FSDT to study the free vibration of a 2D-FG cylindrical shell surrounded by a Winkler–Pasternak elastic foundation. Nguyen et al. [32] introduced the moving Kriging meshfree formulation for the static and free vibration analysis of both square and circular FG plates. Fantuzzi et al. [33] proposed 2D and 3D shell models for the free vibration behaviour of simply supported FG cylindrical and spherical panels. On the basis of a sinusoidal shear deformation theory, Wang and Wu [34] conducted an analysis on the free vibration response of FG porous cylindrical shells. Kant and Punera [35] performed a comprehensive analysis of the static and dynamic behaviour of doubly curved shells. They employed a twelve-variable shear deformation theory by considering the effects of transverse normal strain. Shi and colleagues [36] introduced an enhanced Fourier series method to analyze the free vibrations of FG doubly curved shallow shells with various boundary conditions. They applied an FSDT in conjunction with the Rayleigh-Ritz technique. By employing several equivalent single-layer shell theories, Punera and Kant [37] analysed the free vibration characteristics of FG cylindrical shells. Parand and Alibeigloo [38] provided an analysis of the static and free vibration behaviors of functionally graded sandwich cylindrical shells with a viscoelastic interface using one-dimensional DQM. Khayat et al. [39] employed a semi-analytical finite strip method to examine the free vibration behavior of FG cylindrical shells, considering temperature-dependent properties. Pandey and Pradyumna [40] introduced an innovative high-order layerwise plate finite element formulation intended for static and free vibration analyses of symmetric FGM sandwich plates. Li and co-authors [41] introduced a novel semi-analytical approach for analysing the free vibration of functionally graded porous (FGP) cylindrical shells with arbitrary boundary restraints. Fares and co-authors [42] conducted a static and free vibration analysis of

functionally graded cylindrical and spherical shells, employing an improved layerwise theory. Soviyev and Hui [43] investigated the vibration and stability issues of FG cylindrical shells under external pressure, considering mixed boundary conditions (MBCs) and employing the FSDT. The same authors, in another work [44], investigated the nonlinear free vibration of orthotropic FG cylindrical shells, which interact with two-parametric elastic foundations using FSDT. Based on FSDT and the Rayleigh-Ritz technique, Shi et al. [45] proposed an improved Fourier series method to analyze the free vibrations of functionally graded double curvature shallow shells with various boundary conditions. Zare Jouneghani et al. [46] applied FSDT to investigate the natural vibrations of doubly curved FG shells, including porosities. On the other hand, Pang et al. [47] presented a semi-analytical method for examining the free vibration of stepped FG paraboloidal shells with general edge conditions. The analytical model is constructed using a multi-segment partitioning approach and FSDT.

Li et al. [48, 49] performed a free vibration analysis on doubly-curved functionally graded shells, employing the FSDT and the Ritz method. Tran et al. [50] investigated the thermal vibration behavior of a stiffened FG circular cylindrical shell situated on a Winkler-Pasternak foundation using an FSDT and Lekhnitsky smeared stiffener technique. Similarly, Van Long et al. [51] employed a FSDT to study the nonlinear dynamic response of doubly curved FGM shallow sandwich shells resting on elastic foundations and subjected to underwater explosions. Daikh [52] provided a precise solution for the nonlinear temperature distribution in the context of the free vibration analysis of simply supported FG sandwich plates resting on an elastic foundation. Li et al. [41] introduced a novel semi-analytical approach for analysing the free vibration of FGP cylindrical shells under arbitrary boundary conditions. Arefi and Żur [53] presented a free vibration analysis of an FG cylindrical nanoshell resting on a Pasternak foundation, employing the nonlocal elasticity theory and a two-dimensional approach based on the FSDT. Kushnir et al. [54] investigated analytically the stress-strain state of a finite-length FG cylindrical shell heated by a two-dimensional temperature field, with the material properties varying as analytical functions along the thickness coordinate. Sayyad and Ghugal [55] analysed the static and free vibration of FG singly and doubly curved shells using an analytical solution, based on Navier's technique and generalized higher-order shell theories. By using the finite element method (FEM), Pham and colleagues [56] introduced a shear deformation theory, involving four unknowns, for the bending and hygro-thermo-mechanical vibration of FG sandwich porous doubly curved nanoshells resting on elastic foundation. Shinde and Sayyad [57] formulated a fifth-order shell theory specifically for the static analysis of functionally graded sandwich shells. Vinh and colleagues [58] employed a combination of an FSDT with the modified nonlocal elasticity theory, to examine the free vibration of FG porous doubly curved shallow nanoshells. Belarbi et al. [59] explored the bending and free vibration characteristics of porous FG sandwich plates with diverse porosity distributions, employing an effective layerwise model in their investigation. Hu et al. [60] introduced a novel analytical solution for the free vibration of non-Lévy-type functionally graded doubly curved shallow shells. With the help of Navier's method by using

FEM, Nguyen [61] carried out an analysis of the static bending, free vibration, and buckling response of FG plates resting on Winkler-Pasternak elastic foundations.

Sofiyev and Fantuzzi [62] presented an analytical solution for the stability and vibration problem of clamped cylindrical shells covered by coatings FGM under an axial compressive load. Sayyad and co-authors [63] investigated the static and vibration characteristics of sandwich shells featuring functionally graded face sheets and an isotropic core using higher-order equivalent single-layer shell theories. Ghandourah et al. [64] proposed a novel model known as tri-coated FGM for porous shells structures, which incorporates spatial variations in material properties to analyse the free vibration response. Mouthanna et al. [65] presented innovative approaches encompassing analytical, numerical, and experimental techniques for the nonlinear free vibration analysis of simply supported single-phase FG porous sandwich panels coupled with cylindrical shell panels. This analysis is conducted based on the FSDT. More recently, Daikh et al. [66] developed a quasi-3D analytical plate theory to explore the bending behavior of a new model of FG plate structures resting on modified four parameters Winkler/Pasternak elastic foundations. Later, a ten-node isoparametric triangular element with five degrees of freedom per node is developed by Armendáriz Hernández et al. [67] for the analysis of FG shells. On the other hand, based on Donnell's theory, Deepak et al. [68] carried out a geometrically nonlinear analysis of a simply supported FG doubly curved shell using Kirchhoff's assumption and von Kármán's strain-displacement relationship. Sayyad and Ghugal [55] presented an analytical solution, based on the Navier's technique, for static and free vibration analysis of simply supported doubly curved FGM shells using various equivalent single-layer shell theories with considering the effect of shear deformation and rotary inertia. Rachid et al. [69] applied quasi-3D HSDT, based on Navier's method, to study the bending and free vibration of simply supported cylindrical and spherical FG shells resting on elastic foundations. Pham et al. [70] proposed a smoothed three-node triangular element, based on FSDT, for the static and vibration analyses of FG porous shell structures.

This study addresses a critical research gap by focusing on the dynamic behavior of FG plates and shells, particularly exploring the often-neglected domains of FG spherical, hyperbolic paraboloid, and elliptical paraboloid shells. Despite a wealth of literature on FG cylindrical shells and plates, this emphasis on these less-explored geometries highlights the unique contribution of this work.

A key innovation in this study is the use of an eight-node quadrilateral isoparametric element model, featuring five degrees of freedom per node. Notably, this model incorporates an IFSDT, eliminating the need for a shear correction factor—a typical challenge in evaluating the mechanical properties of functionally graded (FG) structures. This enhancement ensures an accurate representation of shear strain across the material thickness, thereby increasing the fidelity of the analysis. Additionally, the current finite element (FE) model is distinguished by its versatility, as it is capable of analyzing structures with arbitrary boundary conditions and geometries. This flexibility significantly broadens the potential

applications of the research, establishing it as a powerful tool for the examination of a diverse array of structural forms.

Equations of motion are derived through Hamilton's principle, and are solved using the finite element method, producing numerical results for various types of doubly curved shells, including plates, cylinders, spheres, hyperbolic paraboloids, and elliptical paraboloids. Through detailed comparisons with existing studies, the precision and efficiency of the proposed FE model are demonstrated. Furthermore, a comprehensive numerical investigation explores the effects of various parameters on the free vibration behaviors of doubly curved FG shells, providing critical insights that are poised to significantly benefit the engineering community.

2. Theoretical and mathematical formulation:

2.1 Geometrical configuration

Figure 1 depicts a doubly curved shallow shell composed of FGM, characterized by the coordinates (x, y, z). This FGM shell comprises a combination of ceramic and metal elements. The shallow shell exhibits curved dimensions a, b and h in the x, y and z directions, respectively. R_x and R_y denote the principal radii of curvature of the middle plane in the x and y directions, respectively.

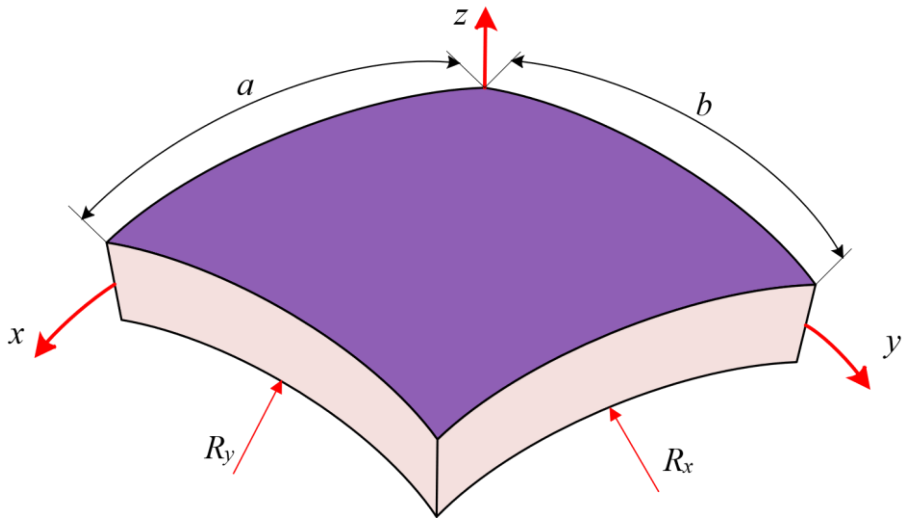

Fig 1. The geometric properties of the doubly curved shells.

Different types of shells structures can be explored in Figure 2 by altering the curvature components of the shells, as demonstrated in table below:

Table 1. Representation of various shell configurations.

Curvature Components	Shell Structure	Abbreviation
$Rx = Ry = \infty$	Flat Plate	FL plate
$R_x = R$, $R_y = \infty$	Cylindrical Shell	CY shell
$R_x = R$, $R_y = R$	Spherical Shell	SP shell
$R_x = R$, $R_y = -R$	Hyperbolic Parabolic Shell	HP shell
$R_x = 1.5R$, $R_y = R$	Elliptical Paraboloid Shell	ELP shell

R stands as a representation denoting the radius of curvature.

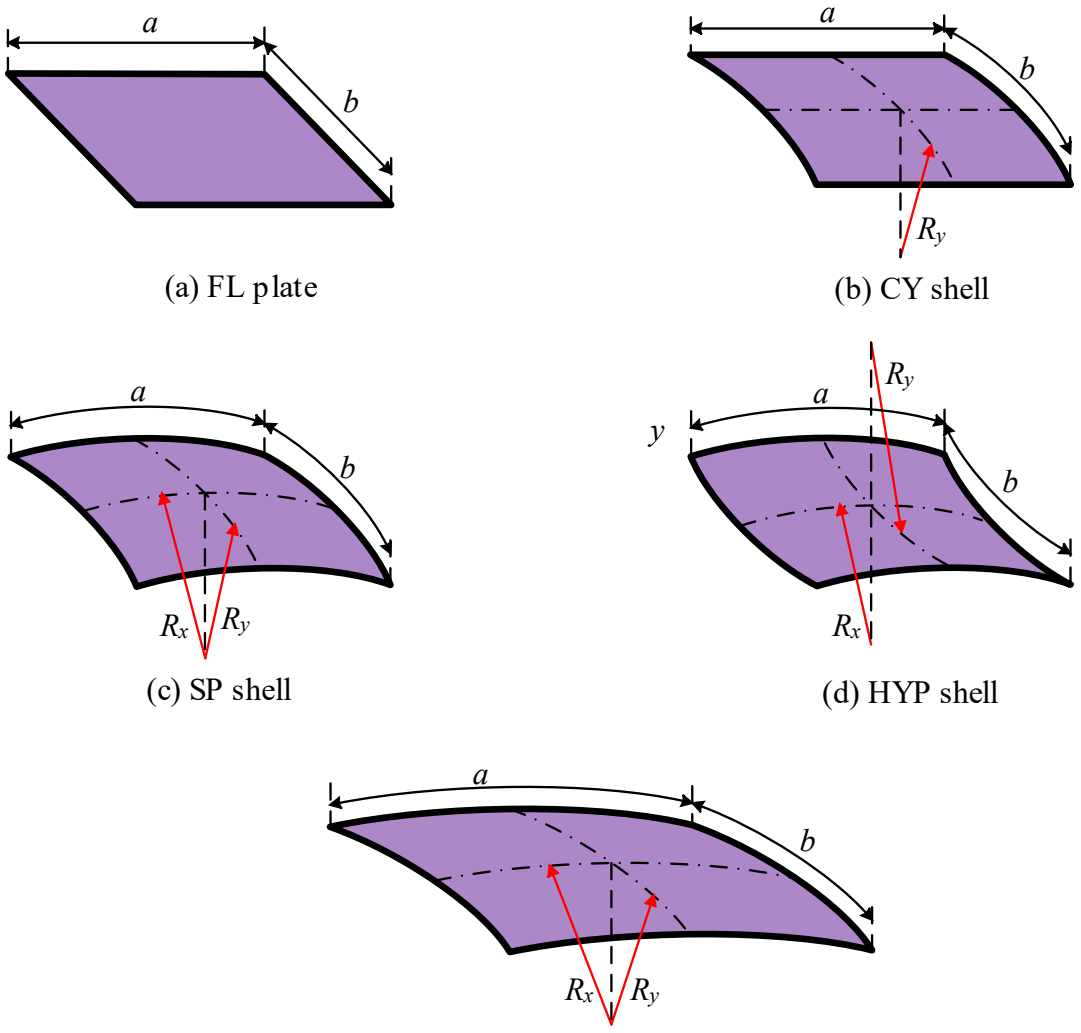

Fig 2. Four types of doubly curved shells.

2.2 Material properties of FGM double-curved shell

The volume fraction within the FGM doubly curved shell changes along the thickness direction according to a power-law function, detailed as follows [68]:

$$\begin{cases} V_c(z) = \left[\frac{z}{h} + \frac{1}{2}\right]^k \\ V_m(z) = 1 - V_c(z) \end{cases} \quad (1)$$

where h is the total thickness of the FGM shell, V_c and V_m are volume fractions of ceramic and metal elements, respectively, and "k" serves as the volume fraction index, allowing for the specification of material property gradation through the shell's thickness direction. The range for "k" is between "0" and "+∞", where a value of "0" signifies a fully ceramic plate, while a value of "+∞" represents a completely metal plate.

The shell, made of functionally graded material combining ceramics and metals, employs the rule of mixture to calculate the effective material properties $P(z)$, such as Young's modulus E (z) and mass density ρ (z), integrating continuous property gradation throughout its thickness.

$$P(z) = P_m + (P_c - P_m)V_c \quad (2)$$

P_m and P_c represent the mechanical properties of the metal and ceramic, respectively. For example, E_c denotes the Young's modulus of the ceramics, and ρ_c is the mass density of the ceramics. E_m denotes the Young's modulus of the metals, and ρ_m is the mass density of the metals.

2.3 Kinematics of the present theory

2.3.1 Displacement field:

In this study, the displacement field for the mentioned FGM double-curved shell is described in accordance with the FSDT as follows:

$$\begin{Bmatrix} u(x,y,z,t) \\ v(x,y,z,t) \\ w(x,y,z,t) \end{Bmatrix} = \begin{Bmatrix} \left(1 + \frac{z}{R_x}\right) u_0(x,y,t) \\ \left(1 + \frac{z}{R_y}\right) v_0(x,y,t) \\ w_0(x,y,t) \end{Bmatrix} + z \begin{Bmatrix} \phi_x(x,y,t) \\ \phi_x(x,y,t) \\ 0 \end{Bmatrix} \quad (3)$$

The variables u, v, and w signify displacements in the x, y, and z directions at any point, while u_0, v_0, and w_0 indicate displacements at the middle plane in the respective directions, with ϕ_x and ϕ_y representing rotations around the x- and y-axes for the transverse normal. Here, time is denoted by t.

2.3.2 Strain-displacement relationships:

For shallow shells, accounting for the impact of curvature components is crucial in determining the strain within the shells. Hence, the strain-displacement relationships for the doubly curved shell are expressed as follows:

$$\begin{cases} \varepsilon_x = \varepsilon_x^0 + z\varepsilon_x^1 \\ \varepsilon_y = \varepsilon_y^0 + z\varepsilon_y^1 \\ \gamma_{xy} = \gamma_{xy}^0 + z\gamma_{xy}^1 \\ \gamma_{xz} = \gamma_{xz}^0 \\ \gamma_{yz} = \gamma_{yz}^0 \end{cases} \tag{4}$$

where:

$$\begin{Bmatrix} \varepsilon_x^0 \\ \varepsilon_y^0 \\ \gamma_{xy}^0 \end{Bmatrix} = \begin{Bmatrix} \frac{\partial u_0}{\partial x} + \frac{w_0}{R_x} \\ \frac{\partial v_0}{\partial y} + \frac{w_0}{R_y} \\ \frac{\partial u_0}{\partial y} + \frac{\partial v_0}{\partial x} \end{Bmatrix}, \qquad \begin{Bmatrix} \varepsilon_x^1 \\ \varepsilon_y^1 \\ \gamma_{xy}^1 \end{Bmatrix} = \begin{Bmatrix} \frac{\partial \phi_x}{\partial x} \\ \frac{\partial \phi_y}{\partial y} \\ \frac{\partial \phi_x}{\partial y} + \frac{\partial \phi_y}{\partial x} \end{Bmatrix}, \begin{Bmatrix} \gamma_{xz}^0 \\ \gamma_{yz}^0 \end{Bmatrix} = \begin{Bmatrix} \frac{\partial w_0}{\partial x} - \frac{u_0}{R_x} + \phi_x \\ \frac{\partial w_0}{\partial y} - \frac{v_0}{R_y} + \phi_y \end{Bmatrix} \tag{5}$$

where ε_x is the longitudinal strain and ε_y is the transverse strain. γ_{xy}, γ_{xz} and γ_{yz} are the shear strains in the *xy*, *xz* and *xz* planes, respectively.

2.4 Constitutive relations:

Disregarding the impact of transverse normal stress (σ_z), the equations governing the behavior of the FG doubly curved shells can be expressed as follows:

$$\begin{Bmatrix} \sigma_{xx} \\ \sigma_{yy} \\ \tau_{xy} \end{Bmatrix} = \begin{bmatrix} Q_{11} & Q_{12} & 0 \\ Q_{21} & Q_{22} & 0 \\ 0 & 0 & Q_{66} \end{bmatrix} \begin{Bmatrix} \varepsilon_{xx} \\ \varepsilon_{yy} \\ \gamma_{xy} \end{Bmatrix} \tag{6}$$

$$\begin{Bmatrix} \tau_{yz} \\ \tau_{xz} \end{Bmatrix} = \begin{bmatrix} Q_{44} & 0 \\ 0 & Q_{55} \end{bmatrix} \begin{Bmatrix} \gamma_{yz} \\ \gamma_{xz} \end{Bmatrix} \tag{7}$$

Where;

$$Q_{11} = Q_{22} = \frac{E(z)}{1-\nu^2}; \qquad Q_{12} = Q_{21} = \frac{\nu E(z)}{1-\nu^2}; \qquad Q_{44} = Q_{55} = Q_{66} = \frac{E(z)}{2(1+\nu)} \tag{8}$$

Here, σ_{xx} and σ_{yy} represents the normal stress in the *x*-direction and *y*-direction, respectively. τ_{xy}, τ_{yz} and τ_{xz} represents the shear stress in the planes, *xy*, *yz* and *xz*, respectively. E represents Youngs modulus, and ν represents the Poisson's ratio.

In numerous structural engineering analyses, the FSDT serves as a common approach, often employing a shear correction factor "k_s" typically set at 5/6. However, this conventional method lacks accuracy in capturing the genuine behavior of transverse shear stresses along the upper and lower surfaces of plates. To address this limitation, a novel and enhanced technique is proposed, substituting the shear correction factor "k_s" with a function $g(z)$ outlined as $g(z) = 5/4 - 5\,z^2/h^2$. Therefore, equation (7) transforms to:

$$\begin{Bmatrix} \tau_{yz} \\ \tau_{xz} \end{Bmatrix} = g(z) \begin{bmatrix} Q_{44} & 0 \\ 0 & Q_{55} \end{bmatrix} \begin{Bmatrix} \gamma_{yz} \\ \gamma_{xz} \end{Bmatrix} \tag{9}$$

The utilization of a parabolic distribution for transverse shear stresses enhances the depiction of stress conditions at shell surfaces, meeting free conditions on both upper and lower surfaces without necessitating a conventional correction factor used in FSDT. This adjustment ensures a realistic and accurate calculation of transverse shear stress variation throughout the shell thickness. The proposed theory offers substantial advantages over current theories, notably in accurately representing the intricate behavior of transverse shear stresses. Our forthcoming numerical study will delve into these details, emphasizing the significant benefits of this innovative theory.

3. Governing differential equation

This analysis utilizes Hamilton's principle to derive the governing equation for the free vibration analyses of FGM doubly curved shells, presented as follows:

$$\delta\Pi = \int_{t_1}^{t_2} \delta(U - T)dt = 0 \tag{10}$$

Here, "t" represents time, while δU and δT denote the variation in strain energy and kinetic energy of the FGM curved shells, respectively. The expression for the first variation of the strain energy is given by:

$$\delta U = \int_V (\sigma_x \delta\varepsilon_x + \sigma_y \delta\varepsilon_y + \tau_{xy}\delta\gamma_{xy} + \tau_{xz}\delta\gamma_{xz} + \tau_{yz}\delta\gamma_{yz})dV \tag{11}$$

$$\delta U = \int_V \left(\sigma_x[\delta\varepsilon_x^0 + z\delta\varepsilon_x^1] + \sigma_y\left[\delta\varepsilon_y^0 + z\delta\varepsilon_y^1\right] + \tau_{xy}\left[\delta\gamma_{xy}^0 + z\delta\gamma_{xy}^1\right] + \tau_{xz}\left[\delta\gamma_{xz}^0 + \tau_{yz}\delta\gamma_{yz}^0\right]\right)dV \tag{12}$$

$$\delta U = \int_A \left(N_x\delta\varepsilon_x^0 + N_y\delta\varepsilon_y^0 + N_{xy}\delta\gamma_{xy}^0 + M_x\delta\varepsilon_x^1 + M_y\delta\varepsilon_y^1 + M_{xy}\delta\gamma_{xy}^1 + Q_{xz}\delta\gamma_{xz}^0 + Q_{yz}\delta\gamma_{yz}^0\right)dA \tag{13}$$

dA and dV represent the infinitesimal area and volume elements, respectively. N_i,M_i,Q_i represent the axial force, bending moment, and shear force, respectively, expressed as:

$$\begin{gathered}\left\{N_x \quad N_y \quad N_{xy} \quad , \quad M_x \quad M_y \quad M_{xy}\right\} = \int_{-\frac{h}{2}}^{\frac{h}{2}} \left\{\sigma_x \quad \sigma_y \quad \tau_{xy} \quad , \quad z\sigma_x \quad z\sigma_y \quad z\tau_{xy}\right\} dz \\ \{Q_{xz} \quad Q_{yz}\} = \int_{-\frac{h}{2}}^{\frac{h}{2}} \{\tau_{xz} \quad \tau_{yz}\} dz\end{gathered} \tag{14}$$

Upon substituting Equations (14) into Equation (11) and integrating across the thickness of the shells, the constitutive equation describing the relationship between force and moment in contact with strain is formulated as:

$$\begin{Bmatrix} N_x \\ N_y \\ N_{xy} \\ M_x \\ M_y \\ M_{xy} \end{Bmatrix} = \begin{bmatrix} A_{11} & A_{12} & 0 & B_{11} & B_{12} & 0 \\ A_{12} & A_{22} & 0 & B_{12} & B_{22} & 0 \\ 0 & 0 & A_{66} & 0 & 0 & B_{66} \\ B_{11} & B_{12} & 0 & D_{11} & D_{12} & 0 \\ B_{12} & B_{22} & 0 & D_{12} & D_{22} & 0 \\ 0 & 0 & B_{66} & 0 & 0 & D_{66} \end{bmatrix} \begin{Bmatrix} \varepsilon_x^0 \\ \varepsilon_y^0 \\ \gamma_{xy}^0 \\ \varepsilon_x^1 \\ \varepsilon_y^1 \\ \gamma_{xy}^1 \end{Bmatrix} \tag{15}$$

$$\begin{bmatrix} Q_{xz} \\ Q_{yz} \end{bmatrix} = \begin{bmatrix} S_{55} & 0 \\ 0 & S_{44} \end{bmatrix} \begin{bmatrix} \gamma_{xz}^0 \\ \gamma_{yz}^0 \end{bmatrix} \tag{16}$$

Where:

$$\left(A_{ij},\, B_{ij},\, D_{ij}\right) = \int_{-\frac{h}{2}}^{\frac{h}{2}} Q_{ij}(z)(1, z,\, z^2)\, dz \quad (i,j = 1,2,6) \tag{17}$$

$$\left(S_{ij}\right) = \int_{-\frac{h}{2}}^{\frac{h}{2}} g(z) Q_{ij}(z)\, dz \qquad (i,j = 4,5) \tag{18}$$

Upon substituting Equation (15) into Equation (13), the expression for the variation of the strain energy can be formulated as follows:

$$\begin{aligned} \delta U = \int_A (&A_{11}\varepsilon_x^0\delta\varepsilon_x^0 + A_{12}\varepsilon_y^0\delta\varepsilon_x^0 + B_{11}\varepsilon_x^1\delta\varepsilon_x^0 + B_{12}\varepsilon_y^1\delta\varepsilon_x^0 + A_{12}\varepsilon_x^0\delta\varepsilon_y^0 + A_{22}\varepsilon_y^0\delta\varepsilon_y^0 \\ &+ B_{12}\varepsilon_x^1\delta\varepsilon_y^0 + B_{22}\varepsilon_y^1\delta\varepsilon_y^0 + A_{66}\gamma_{xy}^0\delta\gamma_{xy}^0 + B_{66}\gamma_{xy}^1\delta\gamma_{xy}^0 + B_{11}\varepsilon_x^0\delta\varepsilon_x^1 \\ &+ B_{12}\varepsilon_y^0\delta\varepsilon_x^1 + D_{11}\varepsilon_x^1\delta\varepsilon_x^1 + D_{12}\varepsilon_y^1\delta\varepsilon_x^1 + B_{12}\varepsilon_x^0\delta\varepsilon_y^1 + B_{22}\varepsilon_y^0\delta\varepsilon_y^1 + D_{12}\varepsilon_x^1\delta\varepsilon_y^1 \\ &+ D_{22}\varepsilon_y^1\delta\varepsilon_y^1 + B_{66}\gamma_{xy}^0\delta\gamma_{xy}^1 + D_{66}\gamma_{xy}^1\delta\gamma_{xy}^1 + \mathrm{A}_{11}^s\gamma_{xz}^0\delta\gamma_{xz}^0 + A_{22}^s\gamma_{yz}^0\delta\gamma_{yz}^0\big)\, dA \end{aligned} \tag{19}$$

The computation of the first variation of kinetic energy for an FGM doubly curved shell follows this formula:

$$\delta T = \int_V \rho(z)\,(\dot{u}\delta\dot{u} + \dot{v}\delta\dot{v} + \dot{w}\delta\dot{w})dV \tag{20}$$

In this equation, $\dot{u}$, $\dot{v}$, and w denote the velocities in the *x*, *y*, and *z* directions, respectively, while *ρ(z)* represents the effective density of the FGM shells at position *z*.

The governing equations of motion for the FG doubly curved shells are derived from Equation (10) as the following set of formulas:

$$\begin{aligned} \frac{\partial N_x}{\partial x} + \frac{\partial N_{xy}}{\partial y} + \frac{Q_x}{R_x} &= I_0\ \ddot{u} + I_1\ \ddot{\phi}_x \\ \frac{\partial N_y}{\partial y} + \frac{\partial N_{xy}}{\partial x} + \frac{Q_y}{R_y} &= I_0\ \ddot{v} + I_1\ \ddot{\phi}_y \\ \frac{\partial Q_x}{\partial x} + \frac{\partial Q_y}{\partial y} - \frac{N_x}{R_x} - \frac{N_y}{R_y} &= I_0\ \ddot{w} \\ \frac{\partial M_x}{\partial x} + \frac{\partial M_{xy}}{\partial y} - Q_x &= I_1\ \ddot{u} + I_2\ \ddot{\phi}_x \\ \frac{\partial M_y}{\partial y} + \frac{\partial M_{xy}}{\partial x} - Q_y &= I_1\ddot{v} + I_2\ \ddot{\phi}_y \end{aligned} \tag{21}$$

The mass moment of inertia coefficients I_0, I_1, I_2 are determined by calculating the following formulas,

$$(I_0, I_1, I_2) = \int_{-\frac{h}{2}}^{\frac{h}{2}} \rho(z)(1, z, z^2)\ dz \tag{22}$$

The computation of the variation in kinetic energy is performed as follows:

$$\delta T = \int_V \begin{bmatrix} \delta\dot{u} & \delta\dot{v} & \delta\dot{w} & \delta\dot{\phi}_x & \delta\dot{\phi}_y \end{bmatrix} \begin{bmatrix} 1 & 0 & 0 & z & 0 \\ & 1 & 0 & 0 & z \\ & & 1 & 0 & 0 \\ & sym & & z^2 & 0 \\ & & & & z^2 \end{bmatrix} \begin{bmatrix} \dot{u} \\ \dot{v} \\ \dot{w} \\ \dot{\phi}_x \\ \dot{\phi}_y \end{bmatrix} \rho(z)\, dV \qquad (23)$$

4. Finite element formulation:

In the present investigation, an efficient C^0 eight-node isoperimetric quadrilateral element with five degrees of freedom per node is developed specifically for the free vibration analysis of FG doubly curved shells (as depicted in Fig. 3). The formulation of this new element is constructed on the foundations of an improved FSDT. In Fig. 3, ξ and η are the natural coordinates system. $x = a$, $x = b$, $y = c$, $y = d$, are the physical coordinates of a point of the element.

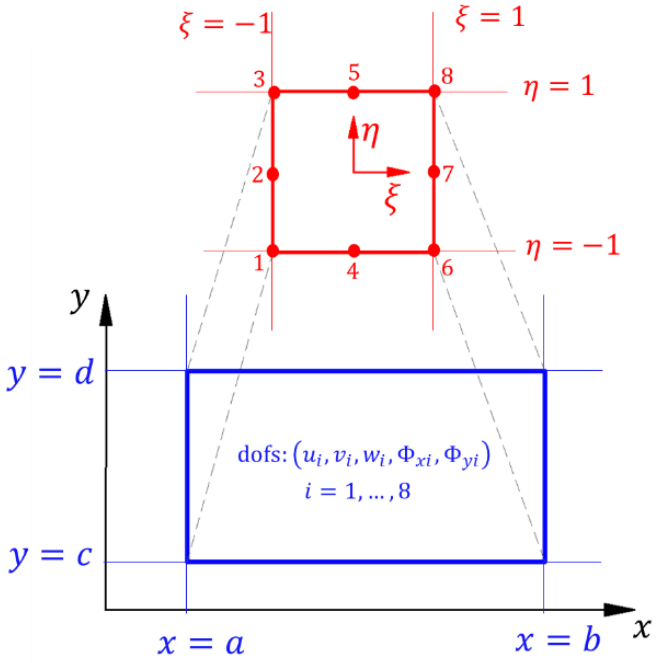

Fig. 3 Geometry and corresponding DOFs of the present element.

The displacement vectors at any point with coordinates (x, y) on the plate are expressed as follows:

$$\delta(x, y) = \sum_{i=1}^{8} N_i\ \delta_i \qquad (24)$$

The displacement vector corresponding to node i (i = 1 to 8) can be written as:

$$\delta_i = \begin{Bmatrix} u_{0i} \\ v_{0i} \\ w_{0i} \\ \phi_{xi} \\ \phi_{yi} \end{Bmatrix}$$

N_i denotes the classical serendipity interpolation functions and is expressed as:

$$
\begin{aligned}
N_1(\xi,\eta) &= -\frac{1}{4}(1-\xi)(1-\eta)(1+\xi+\eta) \quad N_2(\xi,\eta) = -\frac{1}{4}(1+\xi)(1-\eta)(1-\xi+\eta)\\
N_3(\xi,\eta) &= -\frac{1}{4}(1+\xi)(1+\eta)(1-\xi-\eta) \quad N_4(\xi,\eta) = -\frac{1}{4}(1-\xi)(1+\eta)(1+\xi-\eta)\\
N_5(\xi,\eta) &= \frac{1}{2}(1-\xi^2) \quad (1-\eta) \qquad\qquad N_6(\xi,\eta) = \frac{1}{2}(1+\xi)(1-\eta^2)\\
N_7(\xi,\eta) &= \frac{1}{2}(1-\xi^2)(1+\eta) \qquad\qquad N_8(\xi,\eta) = \frac{1}{2}(1-\xi)(1-\eta^2)
\end{aligned}
\tag{25}
$$

By incorporating the shape functions from Equation (25) into the generalized strain vectors outlined in Equation (4), we derive the strain-displacement relationship for each element (*e*) as follows:

$$
\begin{Bmatrix} \varepsilon^0 \\ \varepsilon^1 \\ \gamma^0 \end{Bmatrix}_{(e)} = \begin{bmatrix} B_m \\ B_b \\ B_s \end{bmatrix}_{(e)} \{\delta_i\}_{(e)} \tag{26}
$$

The matrices $[B_m]$, $[B_b]$, and $[B_s]$ establish the relationship between strains and nodal displacements, and they are defined as:

$$
[B_m] = \begin{bmatrix} \frac{\partial N_i}{dx} & 0 & \frac{1}{R_x}N_i & 0 & 0 \\ 0 & \frac{\partial N_i}{dy} & \frac{1}{R_y}N_i & 0 & 0 \\ \frac{\partial N_i}{dy} & \frac{\partial N_i}{dx} & 0 & 0 & 0 \end{bmatrix}
$$

$$
[B_b] = \begin{bmatrix} 0 & 0 & 0 & \frac{\partial N_i}{dx} & 0 \\ 0 & 0 & 0 & 0 & \frac{\partial N_i}{dy} \\ 0 & 0 & 0 & \frac{\partial N_i}{dy} & \frac{\partial N_i}{dx} \end{bmatrix}
$$

$$
[B_s] = \begin{bmatrix} -\frac{1}{R_x}N_i & 0 & \frac{\partial N_i}{dx} & N_i & 0 \\ 0 & -\frac{1}{R_y}N_i & \frac{\partial N_i}{dy} & 0 & N_i \end{bmatrix} \tag{27}
$$

Next, the final free-vibrated FG curved shells motion equation is derived from Eq. (10) and written in the following dynamic equilibrium equation of a system as:

$$
[M]\{\ddot{\delta}\} + [K]\{\delta\} = 0 \tag{28}
$$

where $[M]$ is the global mass matrix, and $[K]$ represents the global elastic stiffness matrix. They are computed using the Gauss numerical integration as follows:

- The global elastic stiffness matrix for the FGM curved shells is calculated as follows:

$$[K] = \sum \int_A \left(\underbrace{[B_m][A][B_m]^T}_{\text{Membrane}} + \underbrace{[B_m][B][B_b]^T}_{\text{Coupling membrane-bending}} + \underbrace{[B_b][B][B_m]^T}_{\text{Coupling bending-membrane}} + \underbrace{[B_b][D][B_b]^T}_{\text{Bending}} + \underbrace{[B_s][S][B_s]^T}_{\text{Shear}} \right) dA \quad (29)$$

- The global mass matrix for the FGM curved shell is calculated as follows:

$$[M] = \sum \int_A ([N_m]^T [I_K][N_m])\ dA \quad (30)$$

Where

$$I_k = \int_{-\frac{h}{2}}^{\frac{h}{2}} \rho(z) \begin{bmatrix} 1 & 0 & 0 & z & 0 \\ & 1 & 0 & 0 & z \\ & & 1 & 0 & 0 \\ & sym & & z^2 & 0 \\ & & & & z^2 \end{bmatrix} dz \quad (31)$$

Now, after evaluating the stiffness and mass matrices for all elements, the governing equations for free vibration analysis of FG doubly curved shell can be stated in the form of generalized eigenvalue problem.

$$[K]_{N\times N}\{\chi\}_{N\times 1} - \omega^2[M]_{N\times N}\{\chi\}_{N\times 1} = 0 \quad (32)$$

where, ω denotes the natural frequency, $[K]$ is the global stiffness matrix with dimension of $N \times N$, $[M]$ is the global mass matrix with the dimension of $N \times N$, $\{\chi\}$ is the $N \times 1$ vector corresponding to the mode shapes, and N is the total number of degrees-of-freedom of the shells. The vector corresponding to the mode shapes of the shells is given by:

$$\{\chi\}_{N\times 1} = \{\delta_1 \quad \delta_2 \quad \delta_3 \cdots \delta_i \cdots \quad \delta_{n-1} \quad \delta_n\}^T \quad (33)$$

The eigenvector $\{\chi\}$ consists of all mode shapes of the shells, including out-of-plane vibration mode shapes and in-plane mode shapes. In cases of in-plane vibration, the transverse displacements of the shells approximate zeros. By using this phenomenon, it can be easy to detect the out-of-plane vibration mode shapes and in-plane vibration mode shapes of the shells.

To allow this system of equations to have non-trivial solutions, the determinant must be set to zero as:

$$det([K] - \omega^2[M]) = 0 \quad (34)$$

5. Numerical results and discussions

This section features multiple numerical examples aimed at highlighting the accuracy and efficacy of the proposed finite element (FE) model. These examples explore the free vibration response exhibited by various types of FG doubly curved shells. The presentation includes comprehensive comparison and convergence studies, drawing comparisons with existing literature. The investigation delves into the influence of diverse materials and geometric parameters, considering arbitrary boundary conditions.

Table 2 illustrates the applied boundary conditions for all examples, while Table 3 details the mechanical properties of the constituents forming the FGM shells.

Table 2. Boundary conditions used in the present study.

Boundary conditions	Abbreviations	Restrained edges
Simply supported	SSSS	$v_0 = w_0 = \phi_y = 0$at $x = \pm a/2$ $u_0 = w_0 = \phi_x = 0$ at $y = \pm b/2$
Clamped	CCCC	$u_0 = v_0 = w_0 = \phi_x = \phi_y = 0$ at $x = \pm a/2$ and $y = \pm b/2$
Clamped-Simply supported	CSCS	$v_0 = w_0 = \phi_y = 0$at $x = \pm$a/2 $u_0 = v_0 = w_0 = \phi_x = \phi_y = 0$ at $y = \pm b/2$
Three edges Clamped and one Simply supported	CSCC	$v_0 = w_0 = \phi_x = \phi_y = 0$ at $x = \pm a/2$ and $y = \pm b/2$ $u_0 = 0$ at $x = -a/2$ and $y = \pm$b/2
Two edges Clamped and two opposite edges Free	CFCF	$u_0 = v_0 = w_0 = \phi_x = \phi_y = 0$ at $x = \pm a/2$ $u_0 = v_0 = w_0 = \phi_x = \phi_y \neq 0$ at $y = \pm b/2$

Table 3. Material properties used in the FG doubly curved shell.

Materials	Properties		
	$E\ (GPa)$	ν	$\rho\ (kg/m^3)$
SUS304	207.78	0.318	8166
Si_3N_4	322.27	0.24	2370
SiC	427	0.17	3100
Al	70	0.3	2707
$(Al_2O_3)_1$	380	0.3	3000
$(Al_2O_3)_2$	380	0.3	3800
ZrO_2	151	0.3	3000

Example 1:

Firstly, the convergence of the present FE model is studied in this subsection. The simple supported FG (Al/Al_2O_3) square plates and doubly curved shells are considered. The present numerical results are also compared with the results of Matsunaga [71], Trinh and Kim [72], Alijani et al. [73], Chorfi and Houmat [74], and Van Vinh and Tounsi [75]. It can be seen that the numerical results, for the dimensionless frequencies $\left(\bar{\omega} = \omega h(\rho_c/E_c)\right)$, are convergence at the mesh 6×6, and close to the published results for all cases of FL FG plates, CY, SP, HYP and ELP FG shells, as presented in Table 4. It is noticed that the solutions of Matsunaga [71], Trinh and Kim [72], Alijani et al. [73], and Van Vinh and Tounsi [75] are achieved via analytical solution, and the results of Chorfi and Houmat [74] are achieved via the *p*-version FEM. Hence, it can be concluded that the present FE model is compatible for free vibration analysis of FG shells.

Continuously, in Table 5, the present FE model will be applied to study the vibration of a clamped FG cylindrical shells panel with various power-law index. The present results are compared with the

solutions of Neves et al. [21], and Pradyumna and Bandyopadhyay [76]. It can be seen that the present results are in good agreement with the available data for all considered modes. Hence, the present FE model can be used to study the vibration behaviors of the FG shells with various power-law indexes.

Table 4. Convergence of dimensionless frequencies of simply supported FG (Al/Al_2O_3) square plates and doubly curved shells ($a = b = 10h$).

Type of Shells	Reference	Model	$\bar{\omega}$				
			$k = 0$	$k = 0.5$	$k = 1$	$k = 4$	$k = 10$
FL Plate ($a/R_x = 0$, $b/R_y = 0$)	Present (2×2)	SQ8-IFSDT	0.0597	0.0509	0.0459	0.0393	0.0374
	Present (4×4)	SQ8-IFSDT	0.0577	0.0491	0.0442	0.0381	0.0364
	Present (6×6)	SQ8-IFSDT	0.0577	0.0490	0.0442	0.0381	0.0364
	Present (8×8)	SQ8-IFSDT	0.0577	0.0490	0.0442	0.0381	0.0364
	Present (10×10)	SQ8-IFSDT	0.0577	0.0490	0.0442	0.0381	0.0364
	Matsunaga [71]	HSDT	0.0588	0.0492	0.0430	0.0381	0.0364
	Trinh and Kim [72]	TSDT	0.0577	0.0490	0.0442	0.0381	0.0364
	Alijani et al. [73]	FSDT	0.0597	0.0506	0.0456	0.0396	0.0380
	Chorfi and Houmat [74]	P-FEM	0.0577	0.0490	0.0442	0.0383	0.0366
	Van Vinh and Tounsi [75]	FSDT	0.0577	0.0490	0.0442	0.0382	0.0366
CY Shells ($a/R_x = 0.5$, $b/R_y = 0$)	Present (2×2)	SQ8-IFSDT	0.0637	0.0546	0.0494	0.0418	0.0394
	Present (4×4)	SQ8-IFSDT	0.0617	0.0528	0.0477	0.0406	0.0383
	Present (6×6)	SQ8-IFSDT	0.0617	0.0527	0.0477	0.0406	0.0383
	Present (8×8)	SQ8-IFSDT	0.0617	0.0527	0.0477	0.0405	0.0383
	Present (10×10)	SQ8-IFSDT	0.0617	0.0527	0.0477	0.0405	0.0383
	Matsunaga [71]	HSDT	0.0622	0.0535	0.0485	0.0413	0.0390
	Trinh and Kim [72]	TSDT	0.0628	0.0538	0.0488	0.0416	0.0392
	Alijani et al. [73]	FSDT	0.0648	0.0553	0.0501	0.0430	0.0408
	Chorfi and Houmat [74]	P-FEM	0.0629	0.0540	0.0490	0.0419	0.0395
	Van Vinh and Tounsi [75]	FSDT	0.0617	0.0527	0.0477	0.0407	0.0385
SP Shells ($a/R_x = 0.5$, $b/R_y = 0.5$)	Present (2×2)	SQ8-IFSDT	0.0764	0.0662	0.0603	0.0501	0.0463
	Present (4×4)	SQ8-IFSDT	0.0746	0.0646	0.0589	0.0490	0.0454
	Present (6×6)	SQ8-IFSDT	0.0746	0.0646	0.0588	0.0490	0.0454
	Present (8×8)	SQ8-IFSDT	0.0746	0.0646	0.0588	0.0490	0.0453
	Present (10×10)	SQ8-IFSDT	0.0746	0.0646	0.0588	0.0490	0.0453
	Matsunaga [71]	HSDT	0.0751	0.0657	0.0601	0.0503	0.0464
	Trinh and Kim [72]	TSDT	0.0761	0.0662	0.0605	0.0506	0.0467
	Alijani et al. [73]	FSDT	0.0779	0.0676	0.0617	0.0519	0.0482
	Chorfi and Houmat [74]	P-FEM	0.0762	0.0664	0.0607	0.0509	0.0471
	Van Vinh and Tounsi [75]	FSDT	0.0746	0.0646	0.0588	0.0490	0.0455
HYP Shells ($a/R_x = 0.5$, $b/R_y = -0.5$)	Present (2×2)	SQ8-IFSDT	0.0574	0.0490	0.0443	0.0378	0.0359
	Present (4×4)	SQ8-IFSDT	0.0548	0.0466	0.0420	0.0362	0.0346
	Present (6×6)	SQ8-IFSDT	0.0548	0.0466	0.0420	0.0362	0.0345
	Present (8×8)	SQ8-IFSDT	0.0548	0.0466	0.0420	0.0362	0.0345
	Present (10×10)	SQ8-IFSDT	0.0548	0.0466	0.0420	0.0362	0.0345
	Matsunaga [71]	HSDT	0.0563	0.0479	0.0432	0.0372	0.0355
	Trinh and Kim [72]	TSDT	0.0577	0.0490	0.0442	0.0381	0.0364
	Alijani et al. [73]	FSDT	0.0597	0.0506	0.0456	0.0396	0.0380
	Chorfi and Houmat [74]	P-FEM	0.0580	0.0493	0.0445	0.0385	0.0368
	Van Vinh and Tounsi [75]	FSDT	0.0548	0.0465	0.0420	0.0363	0.0347
ELP Shells ($a/Rx = 0.5$, $b/Ry = 0.75$)	Present (2×2)	SQ8-IFSDT	0.0839	0.0731	0.0668	0.0550	0.0504
	Present (4×4)	SQ8-IFSDT	0.0822	0.0716	0.0653	0.0540	0.0495
	Present (6×6)	SQ8-IFSDT	0.0821	0.0715	0.0653	0.0540	0.0495
	Present (8×8)	SQ8-IFSDT	0.0821	0.0715	0.0653	0.0540	0.0495
	Present (10×10)	SQ8-IFSDT	0.0821	0.0715	0.0653	0.0540	0.0495

Example 2:

Now, the vibration behaviours of the FG doubly curved shells are examined in this subsection. Various types of curved shells including FL plate, CY shells, SP shells, HYP shells and ELP shells with various type of boundary conditions are considered. The numerical results are given in Table 6. Besides, a comparison of the first five dimensionless frequencies of CY FG shells between the present results and the solutions of Zhao et al. [77] is also presented. According to the comparison, it can be concluded that the results calculated by present FE model are in good agreement with the results of Zhao et al. [77]. The frequencies of the FG shells increase rapidly as the increasing of the mode sequence order for all cases of boundary conditions and types of shells. According to Table 6 and Fig. 4, it is obvious that, for all types of curved shells, the frequencies ($\bar{\bar{\omega}}$) of the CCCC FG shells are the highest one, while the frequencies of the CFCF FG shells are the smallest.

The first six modes of the CY FG shells displacements with different boundary conditions are demonstrated and plotted in Fig. 5. It can be seen that the mode shapes of SSSS, CCCC, CSCS, and CFCF FG shells are symmetric, while the mode shapes of CSCC FG shells are asymmetric. It means the boundary conditions play a significant role on the mode shapes of the vibration behaviors of the shells.

Table 5. First four dimensionless frequencies ($\bar{\bar{\omega}} = \omega a^2\sqrt{12\rho_m(1-\nu^2)/E_m h^2}$**)** of a CCCC FG ($Si_3N_4$/SUS304) cylindrical shells panel with different power law index (k), (a/h = 10, R/a= 10).

Mode	References	Models	$\bar{\bar{\omega}}$				
			k = 0	k= 0.2	k = 2	k = 10	k = ∞
1	Present	SQ8-IFSDT	74.2064	60.3690	40.4269	34.9922	32.5926
	Neves et al. [21]	HSDT	74.2634	60.0061	40.5259	35.1663	32.6108
	Pradyumna and Bandyopadhyay [76]	Q9-HSDT	72.9613	60.0269	39.1457	33.3666	32.0274
2	Present	SQ8-IFSDT	141.5267	115.0536	76.7531	66.2729	61.8705
	Neves et al. [21]	HSDT	141.6779	114.3788	76.9725	66.6482	61.9329
	Pradyumna and Bandyopadhyay [76]	Q9-HSDT	138.5552	113.8806	74.2915	63.2869	60.5546
3	Present	SQ8-IFSDT	141.6957	115.2227	76.8629	66.3558	61.9450
	Neves et al. [21]	HSDT	141.8485	114.5495	77.0818	66.7332	62.0082
	Pradyumna and Bandyopadhyay [76]	Q9-HSDT	138.5552	114.0266	74.3868	63.3668	60.6302
4	Present	SQ8-IFSDT	198.8302	161.6120	107.5698	92.7290	86.6707
	Neves et al. [21]	HSDT	199.1566	160.7355	107.9484	93.3350	86.8160
	Pradyumna and Bandyopadhyay [76]	Q9-HSDT	195.5366	160.6235	104.7687	89.1970	85.1788

Table 6. First five dimensionless frequencies ($\bar{\bar{\omega}} = \omega a^2\sqrt{12\rho_m(1-\nu^2)/E_m h^2}$) of FG ($Si_3N_4$/SUS304) doubly curved shells panel under various type of boundary conditions (a/h = 10, k = 2).

Type of Shells	Mode	Reference	Model	$\bar{\bar{\omega}}$				
				SSSS	CSCC	CSCS	CCCC	CFCF
FL Plate (a/R_x = 0, b/R_y = 0)	1	Present	SQ8-IFSDT	23.6528	36.1157	33.0657	40.3181	25.6117
	2	Present	SQ8-IFSDT	56.3989	68.5756	60.8808	76.8625	29.8642
	3	Present	SQ8-IFSDT	56.3989	74.9086	73.3684	76.8625	47.8664
	4	Present	SQ8-IFSDT	79.9682	102.377	79.9682	107.662	65.3604
	5	Present	SQ8-IFSDT	79.9682	102.699	97.6193	126.939	70.8242
CY Shells (a/R_x = 0.1, b/R_y = 0)	1	Present	SQ8-IFSDT	23.6530	36.1374	33.0557	40.4269	25.8319
		Zhao et al. [77]	FSDT	-	36.0330	32.8530	40.1870	-
	2	Present	SQ8-IFSDT	56.3037	68.4821	60.7875	76.7531	30.0553
		Zhao et al. [77]	FSDT	-	68.4820	60.6470	76.8230	-
	3	Present	SQ8-IFSDT	56.3797	74.8902	73.3373	76.8629	47.9460
		Zhao et al. [77]	FSDT	-	74.8440	73.4110	76.885	-
	4	Present	SQ8-IFSDT	79.9682	102.277	80.0652	107.569	65.2262
		Zhao et al. [77]	FSDT	-	101.793	79.3530	107.423	-
	5	Present	SQ8-IFSDT	80.0652	102.864	97.5094	126.830	70.7460
		Zhao et al. [77]	FSDT	-	102.163	97.3290	127.835	-
SP Shells (a/R_x = 0.1, b/R_y = 0.1)	1	Present	SQ8-IFSDT	23.8382	36.3165	33.2451	40.6112	25.8767
	2	Present	SQ8-IFSDT	56.3361	68.5064	60.8194	76.7678	30.0608
	3	Present	SQ8-IFSDT	56.3361	74.8125	73.2722	76.7678	47.9017
	4	Present	SQ8-IFSDT	80.0652	102.225	80.0652	107.511	65.2350
	5	Present	SQ8-IFSDT	80.0652	102.864	97.4670	126.723	70.7563
HYP Shells (a/R_x = 0.1, b/R_y = -0.1)	1	Present	SQ8-IFSDT	23.6033	36.3027	33.2390	40.5551	25.8690
	2	Present	SQ8-IFSDT	56.3947	68.6470	60.9680	76.9071	30.0583
	3	Present	SQ8-IFSDT	56.435	74.9483	73.3778	76.9432	47.9936
	4	Present	SQ8-IFSDT	79.8713	102.366	80.0652	107.661	65.2964
	5	Present	SQ8-IFSDT	80.0652	102.861	97.5906	126.981	70.7503
ELP Shells (a/R_x = 0.1, b/R_y = 0.15)	1	Present	SQ8-IFSDT	23.9803	36.5336	33.478	40.8192	25.9296
	2	Present	SQ8-IFSDT	56.3037	68.5892	60.9149	76.7148	30.0668
	3	Present	SQ8-IFSDT	56.4136	74.7666	73.2306	76.8382	47.8808
	4	Present	SQ8-IFSDT	80.0652	102.212	80.0652	107.494	65.2690
	5	Present	SQ8-IFSDT	80.1139	102.863	97.4605	126.682	70.7669

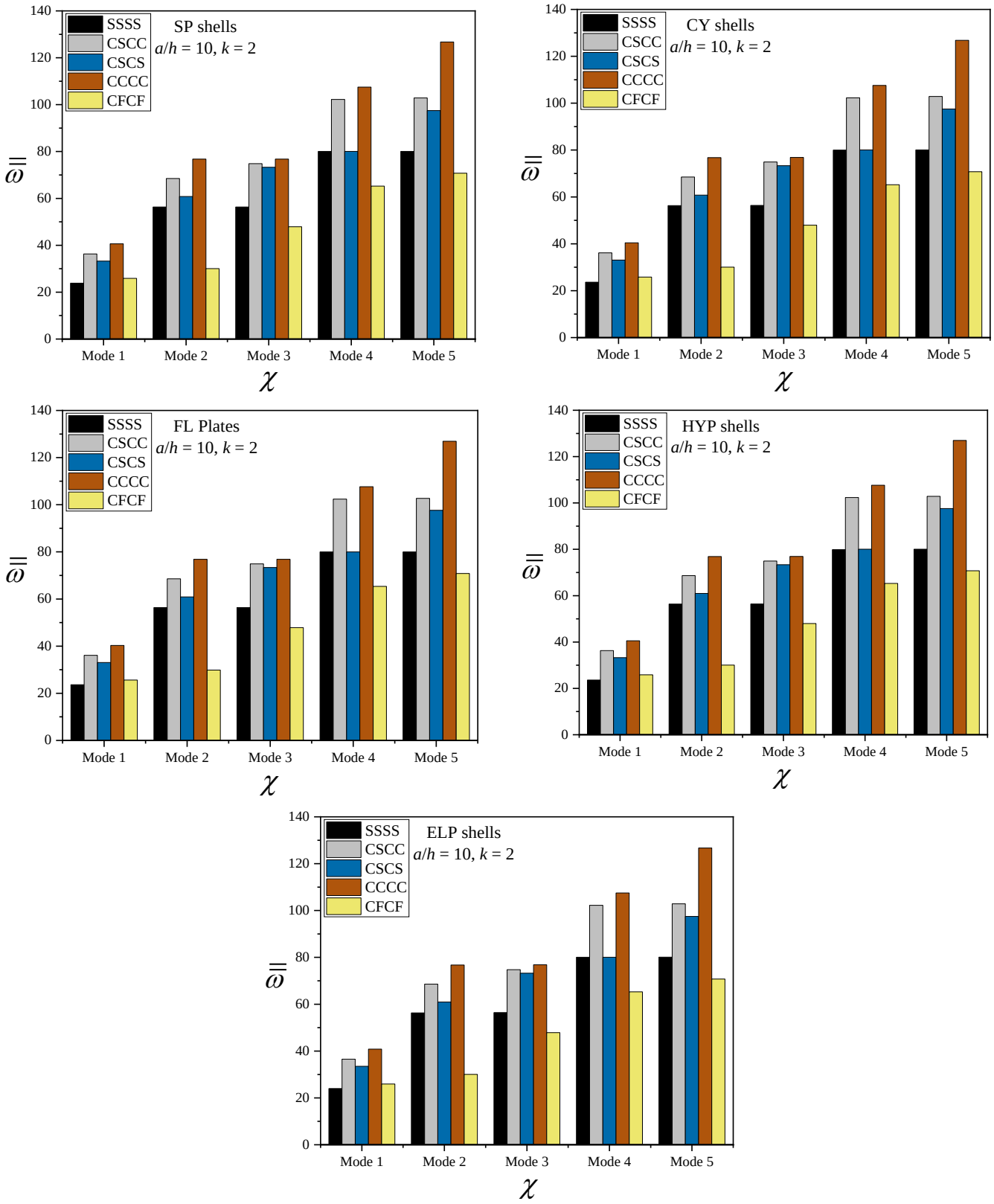

Fig. 4 Effect of mode's number on the dimensionless frequencies of FG (Si_3N_4/SUS304) spherical shells with various type of boundary conditions (a/h = 10, k = 2).

CY Shells : SSSS

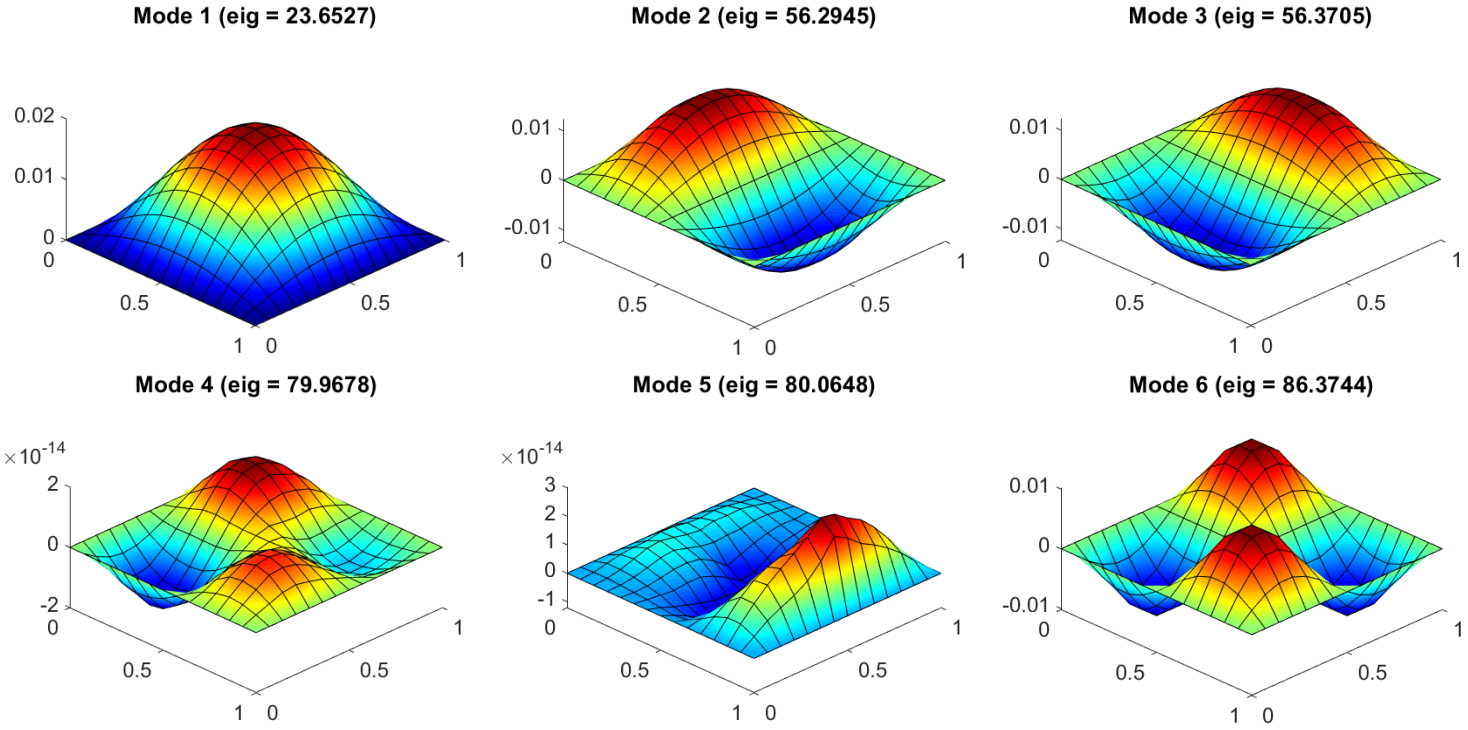

CY Shells : CSCC

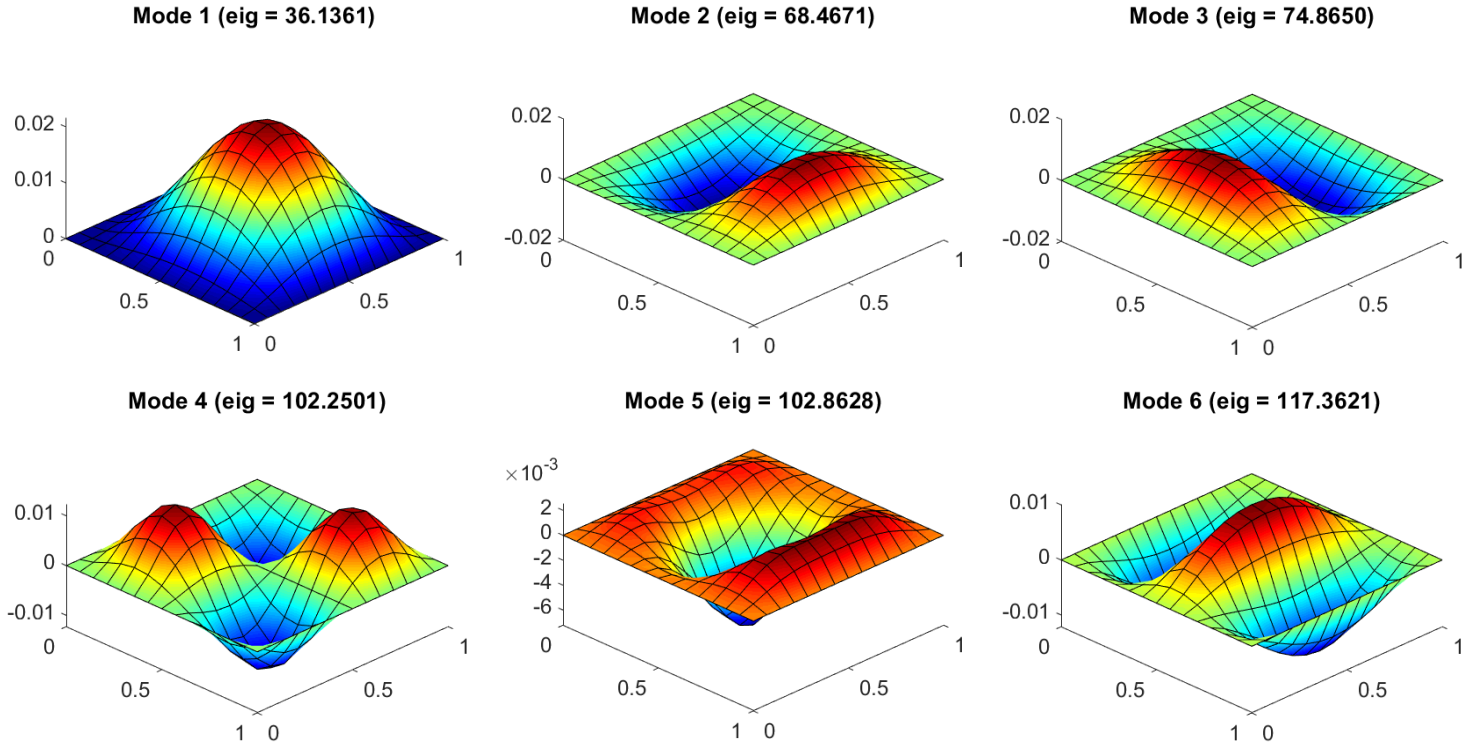

CY Shells : CSCS

Mode 1 (eig = 33.0544)

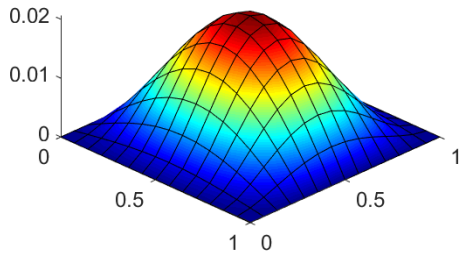

Mode 2 (eig = 60.7787)

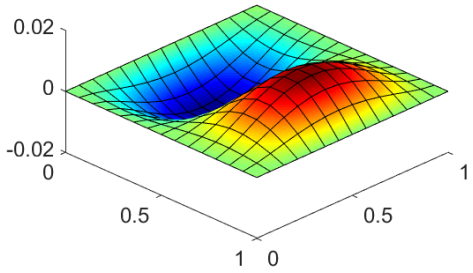

Mode 3 (eig = 73.3116)

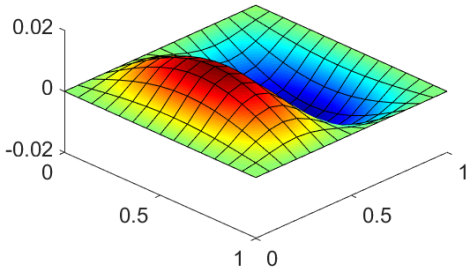

Mode 4 (eig = 80.0648)

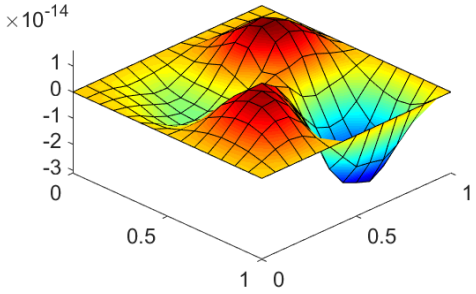

Mode 5 (eig = 97.4846)

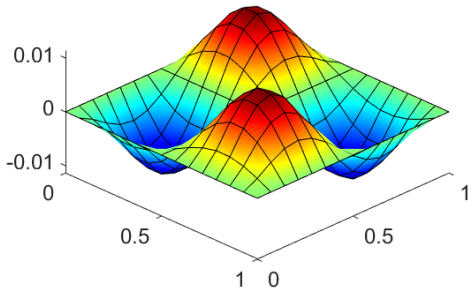

Mode 6 (eig = 107.4334)

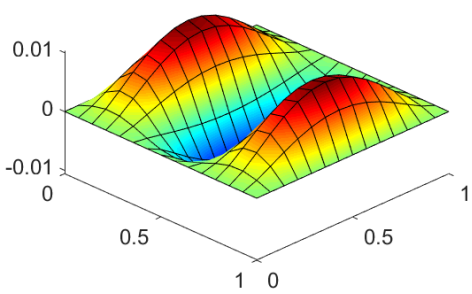

CY Shells : CFCF

Mode 1 (eig = 25.8263)

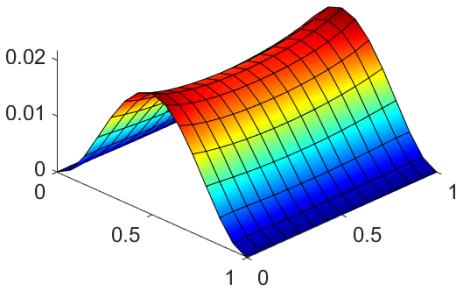

Mode 2 (eig = 30.0467)

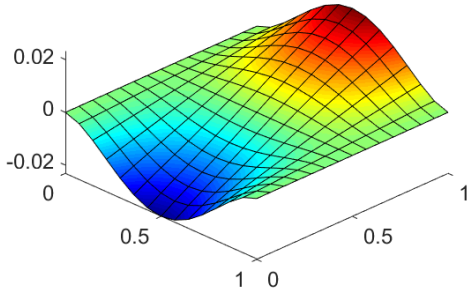

Mode 3 (eig = 47.9346)

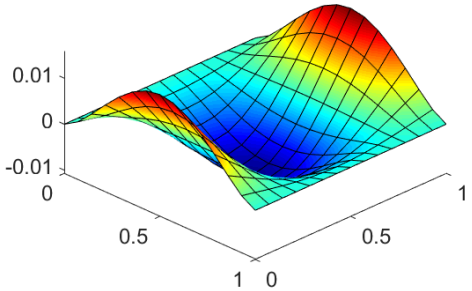

Mode 4 (eig = 65.1883)

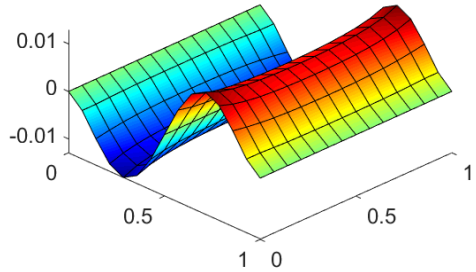

Mode 5 (eig = 70.7027)

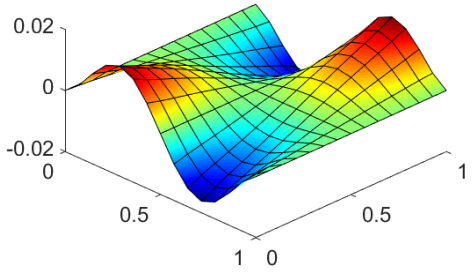

Mode 6 (eig = 72.7360)

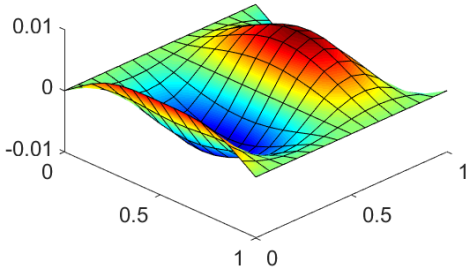

CY Shells : CCCC

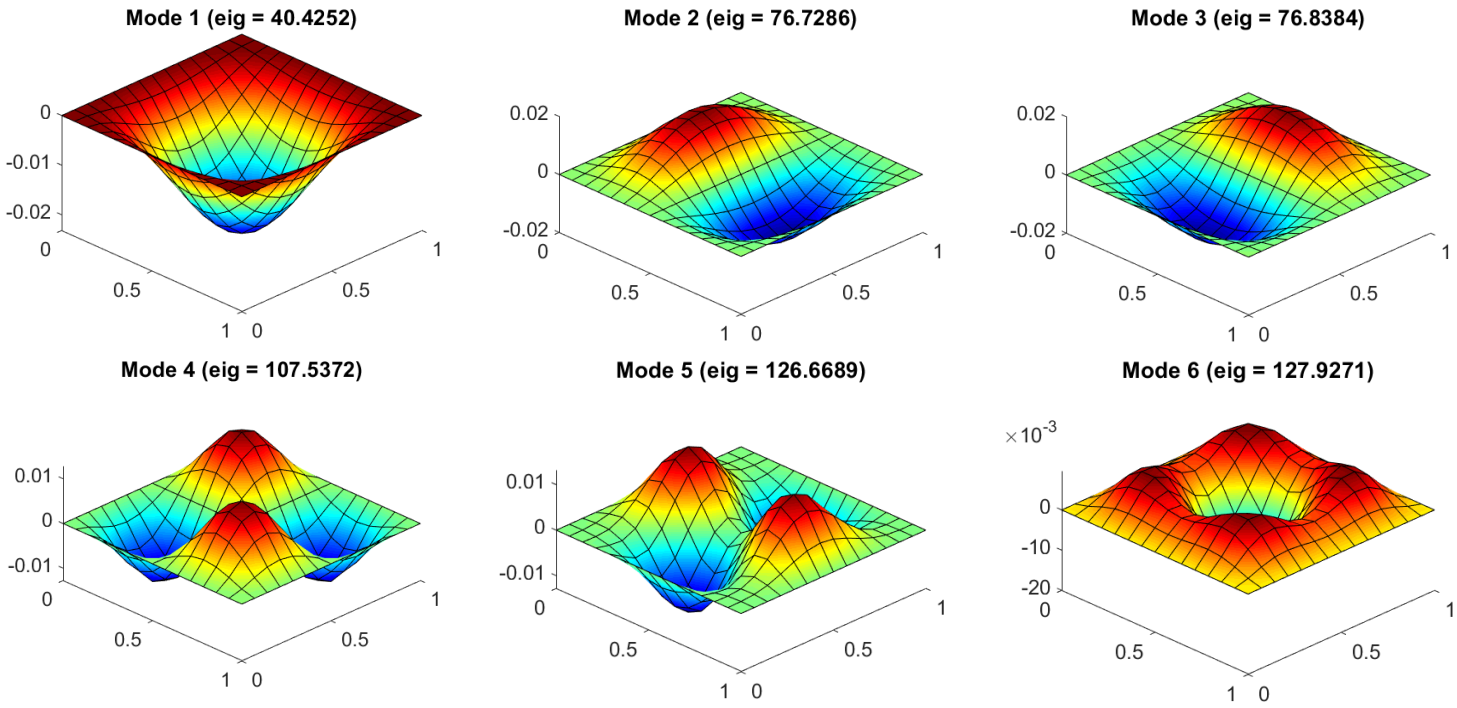

Fig. 5 The first six mode shapes of FG ($SUS304/Si_3N_4$) cylindrical shell under various type of boundary condition (SSSS, CSCC, CSCS, CFCF and CCCC, with k =2, a/R_x = 0.1, b/R_y=0, a/h =10).

Example 3:

As a third example, the natural frequencies ($\bar{\bar{\omega}}$) of the FG (Al/Al_2O_3) CY and SP shells with different radius-to-length ratios are presented, respectively, in Table 7 and Table 8. The computed results are obtained for different values of power law index (k = 0, 0.2, 0.5, 1, 2, 10 and ∞), various radius-to-length ratio (R/a = 0.5, 1, 5, 10, 50 and ∞) and two type of boundary conditions (SSSS and CCCC). The present numerical results are also compared with the available data including the analytical solutions of Neves et al. [21] and the numerical solution (FEM-Q9) of Pradyumna and Bandyopadhyay [78]. According to this comparison, it can be seen that a good agreement is achieved. It was also noticed that the present FE model is developed based on the IFSDT, while the solution of Neves et al. [21] and Pradyumna and Bandyopadhyay [78] are computed via HSDTs. Moreover, according to these tables, it can be seen that the natural frequencies of the FG CY and SP shells decrease when the radius-to-length ratio increases. In general, the frequencies of the FG SP shells are higher than frequencies of FG CY shells with similar radius-to-thickness ratio. In the case of R/a = ∞, the CY and SP shells become as the flat plates, and their frequencies are similar. The frequencies of the flat plates are the limit values of the frequencies of the FG CY and SP shells. Figs. 6 and 7 also present the variation of the frequencies of the FG CY and SP shells with respect to the variation of the radius-to-length ratio in the case of SSSS and CCCC boundary condition. The frequencies of the shells decrease very fast when the radius-to-length ratio

increases from 0.5 to 5, and then the speed of the decrease slows down, and then the frequencies of the shells reach a lower limit. Furthermore, when the power-law index increases, the frequencies of the FG shells decrease. It is noticed that when the power-law index increases, the volume fraction of the ceramic component decreases and the volume fraction of the metal component increases; consequently, the rigidity of the shells decreases. The frequencies of the homogeneous ceramic shells are the highest ones, and the frequencies of the homogeneous metal shells are the smallest ones. Besides, the frequencies of the CCCC shells are higher than the frequencies of the SSSS shells as presented in Figs. 6 and 7.

Example 4:

In this example, the effects of the power-law index (k) on the dimensionless frequencies of the FG (Al/Al_2O_3) shells are presented in Table 9 for thick spherical shells. The side-to-thickness ratio is taken as ($a/h = 5$). The present results are also compared with the available solutions of Neves et al. [26], Fares et al. [42], Sayyad and Ghugal [55], and Pradyumna and Bandyopadhyay [76]. It can be seen that the present results are in excellent agreement with available solutions. In general, when the power-law index increases, the frequencies of the FG shells decrease. The reason is that when the power-law index increases, the FG shells become metal-rich structures, and the rigidity of the shells will decrease. When $k = 0$, the FG shells become homogeneous ceramic shells; therefore, the rigidity of the FG shells is the highest, and the frequencies of the shells are also the highest frequencies. When $k = \infty$, the FG shells become homogeneous metal shells, so the rigidity of the shells will be the smallest, and the frequencies of the shells will be the smallest ones. The effects of the power-law index on the vibration of the different types of FG shells are demonstrated in Table 10. The present results are also compared with the available results of Sayyad and Ghugal [55]. It can be seen that when the power-law index increases, the frequencies of the four types of considered FG shells and FG plates decrease. The reason for this phenomenon is similar to previous results. Table 11 presents the effects of the radius-to-length ratio on the frequencies of the FG shells. When the radius-to-length ratio increases, the frequencies of CY shells, HYP shells increase, while those of SP shells and ELP shells decrease. The values and variations of the frequencies of the FG shells are also compared with the results of Sayyad and Ghugal [55]. The influence of the thickness ratio a/h and power-law index on the frequencies of CCCC FG CY shells is given in Table 12 and Fig. 8. The present results are also compared with the solutions of Neves et al. [26], Fares et al. [42], and Pradyumna and Bandyopadhyay [76], and it can be seen that the present results are in good agreement with the published data. According to Fig. 8, it is obvious that when the power-law index increases, the frequencies of the CY shells decrease rapidly, especially when the power-law index increases from 0 to 2. The phenomenon happens due to the fact that when the power-law index increase, the volume fraction of the ceramic phase decreases and the volume fraction of the metal phase increase, so the rigidity of the shell decreases. On the other hand, the frequencies of the CY shell increase when the ratio a/h increases

Table 7. Effect of the power-law index (k) on the dimensionless frequencies of FG (Al/Al_2O_3) cylindrical shells with various radius-to-length ratio (R/a), (a/h = 10, $R_x = R$, $R_y = \infty$)

k	BCs	References	Models	$\bar{\bar{\omega}}$					
				R/a = 0.5	R/a = 1	R/a = 5	R/a = 10	R/a = 50	Plate
0	SSSS	Present	SQ8-IFSDT	70.2768	52.3676	42.6816	42.3181	42.2008	42.1959
		Neves et al. [21]	HSDT	70.1594	52.1938	42.6701	42.3153	42.2008	42.1961
		Pradyumna and Bandyopadhyay [78]	Q9-HSDT	68.8645	51.5216	42.2543	41.9080	41.7963	41.7917
	CCCC	Present	SQ8-IFSDT	132.9793	95.6351	73.1096	72.2699	71.9989	71.9876
		Neves et al. [21]	HSDT	133.6037	95.5849	73.1640	72.3304	72.0614	72.0502
		Pradyumna and Bandyopadhyay [78]	Q9-HSDT	129.9808	94.4973	71.8861	71.0394	70.7660	70.7546
0.2	SSSS	Present	SQ8-IFSDT	65.4511	48.3040	39.0263	38.6865	38.5837	38.5817
		Neves et al. [21]	HSDT	65.3889	47.9338	38.7168	38.3840	38.2842	38.2827
		Pradyumna and Bandyopadhyay [78]	Q9-HSDT	64.4001	47.5968	40.1621	39.8472	39.7465	39.7426
	CCCC	Present	SQ8-IFSDT	122.1349	88.4132	67.1132	66.3258	66.0791	66.0714
		Neves et al. [21]	HSDT	121.8612	87.8148	66.6620	65.8808	65.6371	65.6299
		Pradyumna and Bandyopadhyay [78]	Q9-HSDT	119.6109	87.3930	68.1152	67.3320	67.0801	67.0698
0.5	SSSS	Present	SQ8-IFSDT	60.1472	43.8757	35.0463	34.7303	34.6411	34.6419
		Neves et al. [21]	HSDT	60.4255	43.6883	34.8768	34.5672	34.4809	34.4820
		Pradyumna and Bandyopadhyay [78]	Q9-HSDT	59.4396	43.3019	37.2870	36.9995	36.9088	36.9057
	CCCC	Present	SQ8-IFSDT	110.1514	80.4596	60.4870	59.7537	59.5311	59.5268
		Neves et al. [21]	HSDT	110.2017	80.0146	60.2477	59.5215	59.3022	59.2985
		Pradyumna and Bandyopadhyay [78]	Q9-HSDT	108.1546	79.5689	63.1896	62.4687	62.2380	62.2291
1	SSSS	Present	SQ8-IFSDT	54.3333	39.2196	31.0007	30.7130	30.6377	30.6407
		Neves et al. [21]	HSDT	54.8909	39.1753	30.9306	30.6485	30.5759	30.5792
		Pradyumna and Bandyopadhyay [78]	Q9-HSDT	53.9296	38.7715	33.2268	32.9585	32.8750	32.8726
	CCCC	Present	SQ8-IFSDT	97.5381	71.9929	53.6108	52.9399	52.7427	52.7413
		Neves et al. [21]	HSDT	97.9069	71.6716	53.5430	52.8800	52.6864	52.6856
		Pradyumna and Bandyopadhyay [78]	Q9-HSDT	96.0666	71.2453	56.5546	55.8911	55.6799	55.6722
2	SSSS	Present	SQ8-IFSDT	48.0327	34.6997	27.5296	27.2868	27.2288	27.2335
		Neves et al. [21]	HSDT	48.7807	34.7654	27.5362	27.2979	27.2423	27.2472
		Pradyumna and Bandyopadhyay [78]	Q9-HSDT	47.8259	34.3338	27.4449	27.1789	27.0961	27.0937
	CCCC	Present	SQ8-IFSDT	85.6285	63.6310	47.4525	46.8691	46.7030	46.7039
		Neves et al. [21]	HSDT	86.3088	63.4398	47.5205	46.9447	46.7820	46.7835
		Pradyumna and Bandyopadhyay [78]	Q9-HSDT	84.4431	62.9748	36.2487	35.6633	35.4745	35.4669

Table 7. Continued

k	BCs	References	Models	R/a = 0.5	R/a = 1	R/a = 5	R/a = 10	R/a = 50	Plate
10	SSSS	Present	SQ8-IFSDT	37.6144	28.6359	24.0993	23.9541	23.9217	23.9253
		Neves et al. [21]	HSDT	38.2792	28.8072	24.2472	24.1063	24.0762	24.0802
		Pradyumna and Bandyopadhyay [78]	Q9-HSDT	37.2593	28.2757	19.3892	19.1562	19.0809	19.0778
	CCCC	Present	SQ8-IFSDT	70.8227	51.9144	40.5104	40.1104	39.9959	39.9962
		Neves et al. [21]	HSDT	71.7634	52.0900	40.8099	40.4145	40.3028	40.3037
		Pradyumna and Bandyopadhyay [78]	Q9-HSDT	69.8224	51.3803	33.6611	33.1474	32.9812	32.9743
∞	SSSS	Present	SQ8-IFSDT	31.7979	23.7119	19.3437	19.1800	19.1273	19.1252
		Neves et al. [21]	HSDT	31.7000	23.5827	19.2796	19.1193	19.0675	19.0654
		Pradyumna and Bandyopadhyay [78]	Q9-HSDT	31.9866	24.1988	19.0917	18.9352	18.8848	18.8827
	CCCC	Present	SQ8-IFSDT	60.2024	43.2974	33.1225	32.7435	32.6213	32.6162
		Neves et al. [21]	HSDT	60.3660	43.1880	33.0576	32.6810	32.5594	32.5543
		Pradyumna and Bandyopadhyay [78]	Q9-HSDT	61.0568	44.2962	32.4802	32.0976	31.9741	31.9689

Table 8. Effect of the power-law index (k) on the dimensionless frequencies of FG (Al/Al_2O_3) spherical shells with various radius-to-length ratio (R/a), ($a/h = 10$, $R_x = R_y = R$)

k	BCs	References	Models	$\overline{\overline{\omega}}$					
				$R/a = 0.5$	$R/a = 1$	$R/a = 5$	$R/a = 10$	$R/a = 50$	Plate
0	SSSS	Present	SQ8-IFSDT	125.9402	79.1503	44.4425	42.7701	42.2190	42.1959
		Neves et al. [21]	HSDT	126.2994	79.2626	44.4455	42.7709	42.2192	42.1961
		Pradyumna and Bandyopadhyay [78]	Q9-HSDT	124.1581	78.2306	44.0073	42.3579	41.8145	41.7917
	CCCC	Present	SQ8-IFSDT	176.4617	122.0283	74.7629	72.6923	72.0159	71.9876
		Neves et al. [21]	HSDT	176.8125	122.0934	74.8207	72.7536	72.0784	72.0502
		Pradyumna and Bandyopadhyay [78]	Q9-HSDT	173.9595	120.9210	73.5550	71.4659	70.7832	70.7546
0.2	SSSS	Present	SQ8-IFSDT	117.3811	73.4592	40.6879	39.1067	38.5984	38.5817
		Neves et al. [21]	HSDT	117.3053	73.2663	40.3936	38.8074	38.2988	38.2827
		Pradyumna and Bandyopadhyay [78]	Q9-HSDT	115.7499	72.6343	41.7782	40.2608	39.7629	39.7426
	CCCC	Present	SQ8-IFSDT	163.5725	113.1691	68.6616	66.7140	66.0922	66.0714
		Neves et al. [21]	HSDT	163.0852	112.7143	68.2142	66.2686	65.6498	65.6299
		Pradyumna and Bandyopadhyay [78]	Q9-HSDT	161.3704	112.2017	69.6597	67.7257	67.0956	67.0698
0.5	SSSS	Present	SQ8-IFSDT	107.9893	67.2395	36.6030	35.1180	34.6525	34.6419
		Neves et al. [21]	HSDT	108.0044	67.1623	36.4453	34.9574	34.4922	34.4820
		Pradyumna and Bandyopadhyay [78]	Q9-HSDT	106.5014	66.5025	38.7731	37.3785	36.9234	36.9057
	CCCC	Present	SQ8-IFSDT	149.3293	103.4264	61.9270	60.1076	59.5406	59.5268
		Neves et al. [21]	HSDT	149.0931	103.1804	61.6902	59.8745	59.3112	59.2985
		Pradyumna and Bandyopadhyay [78]	Q9-HSDT	147.4598	102.5983	64.6114	62.8299	62.2519	62.2291
1	SSSS	Present	SQ8-IFSDT	97.5959	60.5004	32.4299	31.0637	30.6460	30.6407
		Neves et al. [21]	HSDT	97.6938	60.5121	32.3691	31.0012	30.5840	30.5792
		Pradyumna and Bandyopadhyay [78]	Q9-HSDT	96.2587	59.8521	34.6004	33.3080	32.8881	32.8726
	CCCC	Present	SQ8-IFSDT	133.8674	92.9025	54.9262	53.2568	52.7489	52.7413
		Neves et al. [21]	HSDT	133.8751	92.8282	54.8597	53.1956	52.6921	52.6856
		Pradyumna and Bandyopadhyay [78]	Q9-HSDT	132.3396	92.2147	57.8619	56.2222	55.6923	55.6722
2	SSSS	Present	SQ8-IFSDT	86.0033	53.3588	28.7678	27.5853	27.2340	27.2335
		Neves et al. [21]	HSDT	86.2288	53.4659	28.7833	27.5984	27.2474	27.2472
		Pradyumna and Bandyopadhyay [78]	Q9-HSDT	84.8206	52.7875	28.7459	27.5110	27.1085	27.0937
	CCCC	Present	SQ8-IFSDT	117.7538	81.9981	48.5959	47.1391	46.7064	46.7039
		Neves et al. [21]	HSDT	118.0167	82.0948	48.6656	47.2135	46.7849	46.7835
		Pradyumna and Bandyopadhyay [78]	Q9-HSDT	116.4386	81.3963	37.3914	35.9568	35.4861	35.4669

Table 8. Continued

10	SSSS	Present	SQ8-IFSDT	66.1520	42.1234	24.9188	24.1492	23.9247	23.9253
		Neves et al. [21]	HSDT	66.7088	42.4365	25.0772	24.3034	24.0791	24.0802
		Pradyumna and Bandyopadhyay [78]	Q9-HSDT	65.2296	41.6702	20.4691	19.4357	19.0922	19.0778
	CCCC	Present	SQ8-IFSDT	93.1927	65.3824	41.2994	40.2967	39.9986	39.9962
		Neves et al. [21]	HSDT	93.9111	65.8103	41.6016	40.5998	40.3049	40.3037
		Pradyumna and Bandyopadhyay [78]	Q9-HSDT	92.1387	64.8773	34.6658	33.4057	32.9916	32.9743
∞	SSSS	Present	SQ8-IFSDT	56.9618	35.8132	20.1382	19.3838	19.1355	19.1252
		Neves et al. [21]	HSDT	57.0657	35.8131	20.0818	19.3251	19.0759	19.0654
		Pradyumna and Bandyopadhyay [78]	Q9-HSDT	57.2005	36.2904	19.8838	19.1385	18.8930	18.8827
	CCCC	Present	SQ8-IFSDT	79.8423	55.2251	33.8687	32.9340	32.6289	32.6162
		Neves et al. [21]	HSDT	79.8889	55.1653	33.8061	32.8722	32.5671	32.5543
		Pradyumna and Bandyopadhyay [78]	Q9-HSDT	80.7722	56.2999	33.2343	32.2904	31.9819	31.9689

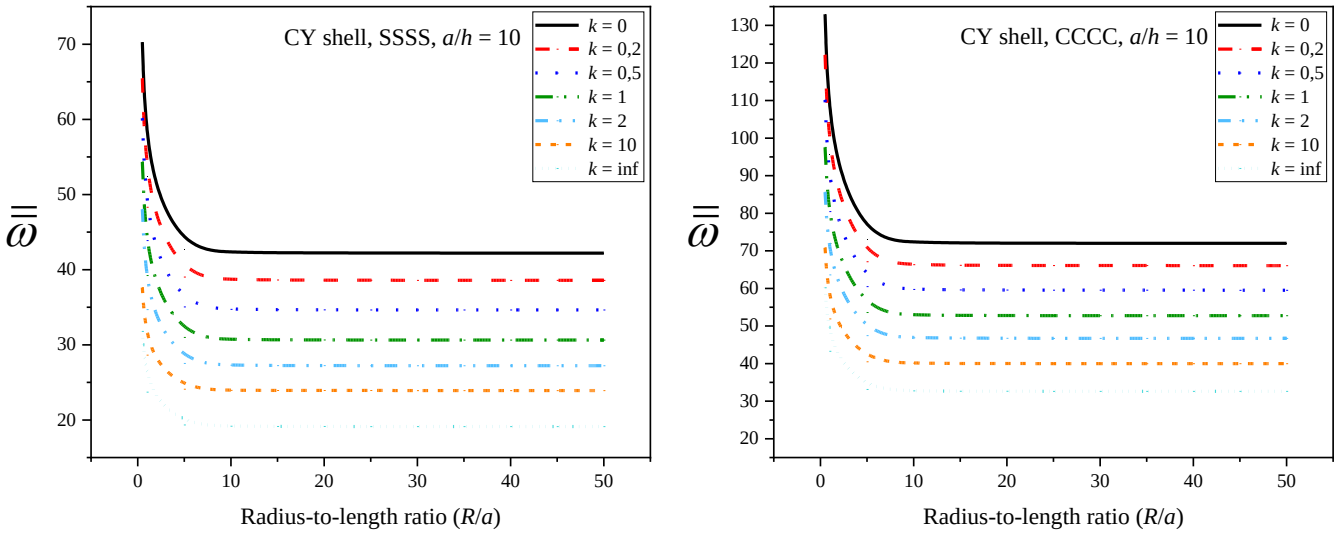

Fig. 6 Effect of radius-to-length ratio (R/a) on the dimensionless frequencies of FG (Al/Al_2O_3) cylindrical shells with various power law index (k), (a/h = 10).

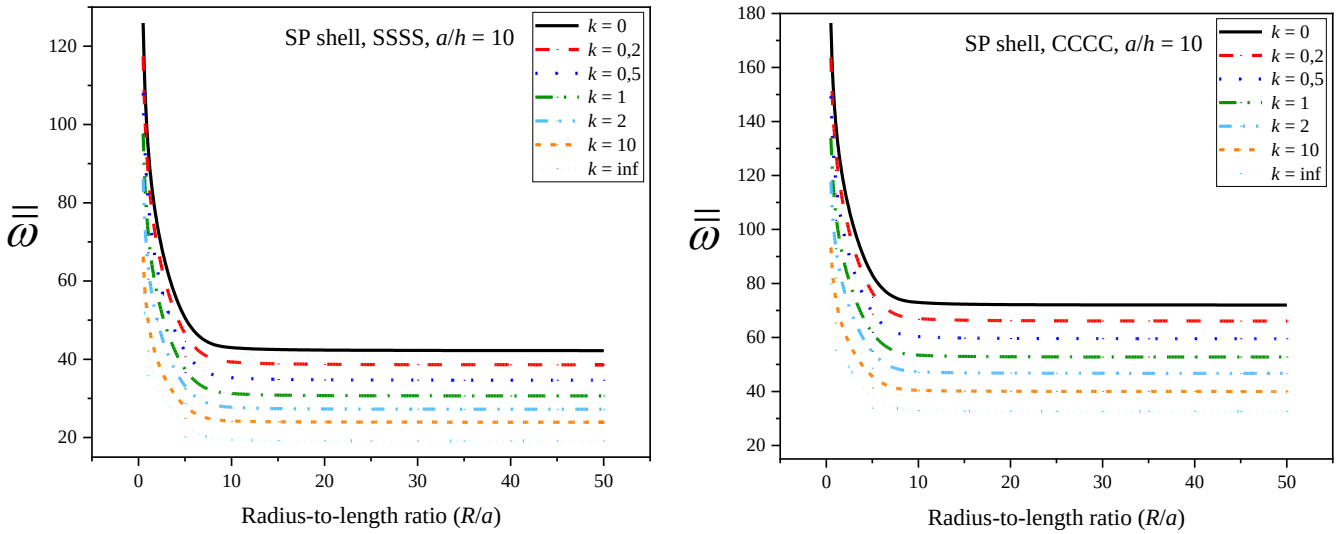

Fig. 7 Effect of radius-to-length ratio (R/a) on the dimensionless frequencies of FG (Al/Al_2O_3) spherical shells with various power law index (k), (a/h = 10).

Table 9. Effects of the power-law index (k) on the dimensionless frequencies ($\bar{\bar{\omega}} = \omega a^2\sqrt{12\rho_m(1-\nu^2)/E_m h^2}$) of FG ($Al/Al_2O_3$) spherical shells ($a = b$, $a/h = 10$).

R_x/a	R_y/b	References	Models	$\bar{\bar{\omega}}$				
				$k = 0$	$k = 1$	$k = 2$	$k = 10$	$k = \infty$
1	1	Present	SQ8-IFSDT	79.1503	60.5004	53.3588	42.1234	35.8132
		Neves et al. [21]	HSDT	79.2626	60.5121	53.4659	42.4365	35.8131
		Fares et al. [37]	LW-FSDT	-	61.1339	53.9021	42.3232	-
		Sayyad and Ghugal [50]	FSDT	80.7278	61.6277	54.3885	43.1749	36.4940
			HSDT	80.6496	61.5875	54.3427	43.0656	36.4586
		Pradyumna and Bandyopadhyay [76]	HSDT	-	59.8521	52.7875	41.6702	-
5	5	Present	SQ8-IFSDT	44.4425	32.4299	28.7678	24.9188	20.1382
		Neves et al. [21]	HSDT	44.4455	32.3691	28.7833	25.0772	
		Fares et al. [37]	LW-FSDT	-	32.5494	28.8368	24.6444	-
		Sayyad and Ghugal [50]	FSDT	44.7919	32.7308	29.0914	25.3157	20.2496
			HSDT	44.6271	32.6273	28.9656	25.0724	20.1751
		Pradyu mna and Bandyopadhyay [76]	HSDT	-	34.6004	28.7459	20.4691	-
10	10	Present	SQ8-IFSDT	42.7701	31.0637	27.5853	24.1492	19.3838
		Neves et al. [21]	HSDT	42.7709	31.0012	27.5984	24.3034	19.3251
		Fares et al. [37]	LW-FSDT	-	31.1043	27.5692	23.8077	—
		Sayyad and Ghugal [50]	FSDT	43.0456	31.2826	27.8307	24.4868	19.4602
			HSDT	42.8732	31.1729	27.6972	24.2324	19.3822
		Pradyumna and Bandyopadhyay [76]	HSDT	-	33.3080	27.5110	19.4357	-
50	50	Present	SQ8-IFSDT	42.2190	30.6460	27.2340	23.9247	19.1350
		Neves et al. [21]	HSDT	42.2192	30.5840	27.2474	24.0791	19.0759
		Fares et al. [37]	LW-FSDT	—	30.6378	27.1630	23.5415	—
		Sayyad and Ghugal [50]	FSDT	42.4696	30.8208	27.4344	24.2300	19.1998
			HSDT	42.2946	30.7088	27.2979	23.9713	19.1207
		Pradyumna and Bandyopadhyay [76]	HSDT	-	32.8881	27.1085	19.0922	-

Table 10. Effects of the power-law index (k) on the dimensionless frequencies, $\left(\bar{\omega} = \omega h(\rho_c/E_c)\right)$, of thick FG ($Al/Al_2O_3$) doubly curved shells panel ($a = b$, $a/h = 5$).

Type of shells	References	Models	$\bar{\omega}$				
			$k = 0$	$k = 1$	$k = 5$	$k = 10$	$k = \infty$
CY Shells ($Rx/a = 5$, $Ry/b = \infty$)	Present	SQ8-IFSDT	0.21139	0.16268	0.13528	0.12942	0.10779
	Sayyad and Ghugal [50]	FSDT	0.21482	0.16546	0.14013	0.13458	0.10953
		HSDT	0.21199	0.16352	0.13600	0.13019	0.10809
SP Shells ($R_x/a = 5$, $R_y/b = 5$)	Present	SQ8-IFSDT	0.21387	0.16429	0.13622	0.13031	0.10904
	Sayyad and Ghugal [50]	FSDT	0.21744	0.16748	0.14142	0.13574	0.11086
		HSDT	0.21465	0.16558	0.13738	0.13143	0.10944
HYP Shells ($R_x/a = 5$, $R_y/b = -5$)	Present	SQ8-IFSDT	0.20927	0.16159	0.13461	0.12866	0.10671
	Sayyad and Ghugal [50]	FSDT	0.21333	0.16452	0.13955	0.13400	0.10877
		HSDT	0.21050	0.16256	0.13537	0.12957	0.10732
ELP Shells ($R_x/a = 5$, $R_y/b = 7.5$)	Present	SQ8-IFSDT	0.21301	0.16370	0.13588	0.13000	0.10861
	Sayyad and Ghugal [50]	FSDT	0.21644	0.16669	0.14091	0.13530	0.11036
		HSDT	0.21364	0.16478	0.13684	0.13095	0.10893
FL Plates ($R_x/a = \infty$, $R_y/b = \infty$)	Present	SQ8-IFSDT	0.21121	0.16303	0.13583	0.12986	0.10770
	Sayyad and Ghugal [50]	FSDT	0.21424	0.16521	0.14014	0.13458	0.10924
		HSDT	0.21139	0.16324	0.13595	0.13014	0.10779

Table 11. Effect of the radius-to-length ratio on the dimensionless frequencies $\left(\overline{\omega} = \omega h(\rho_c/E_c)\right)$ of thick FG (Al/Al_2O_3) doubly curved shells *(a = b, a/h* = 5, *k* = 2).

Type of shells	R_x/a	R_y/b	$\overline{\omega}$		
			Present	Sayyad and Ghugal [50]	
			SQ8-IFSDT	FSDT	HSDT
CY Shells	5	∞	0.14657	0.14996	0.14760
	10	∞	0.14675	0.14978	0.14739
	20	∞	0.14689	0.14978	0.14739
	50	∞	0.14699	0.14981	0.14741
	100	∞	0.14703	0.14983	0.14743
SP Shells	5	5	0.14785	0.15167	0.14936
	10	10	0.14689	0.15012	0.14775
	20	20	0.14683	0.14982	0.14743
	50	50	0.14694	0.14980	0.14740
	100	100	0.14699	0.14982	0.14741
HYP Shells	5	-5	0.14577	0.14922	0.14683
	10	-10	0.14674	0.14969	0.14729
	20	-20	0.14698	0.14981	0.14740
	50	-50	0.14705	0.14984	0.14744
	100	-100	0.14706	0.14985	0.14744
ELP Shells	5	7.5	0.14737	0.15100	0.14867
	10	15	0.14683	0.14998	0.14760
	20	30	0.14685	0.14980	0.14741
	50	75	0.14695	0.14980	0.14740
	100	150	0.14700	0.14982	0.14742

Table 12. Dimensionless frequencies $\left(\bar{\omega} = \omega h(\rho_c/E_c)\right)$ of CCCC FG (Al/Al_2O_3) cylindrical shell for different side-to-thickness ratios (a/h) and k. (a/R= 0.1).

k	References	Models	$\bar{\omega}$					
			a/h =5	a/h =10	a/h =15	a/h =20	a/h =50	a/h =100
0	Present	SQ8-IFSDT	58.7906	72.2699	76.4775	78.4950	85.6155	102.4167
	Neves et al. [21]	HSDT	59.0433	72.3272	76.4904	78.4918	85.6073	102.3351
	Fares et al. [37]	LW-FSDT	60.6930	73.1994	76.2482	77.2742	86.3801	103.5890
	Pradyumna and Bandyopadhyay [78]	Q9-HSDT	58.2858	71.7395	75.0439	77.0246	84.8800	102.9227
0.5	Present	SQ8-IFSDT	49.3529	59.7537	62.9578	64.5334	70.7172	85.8410
	Neves et al. [21]	HSDT	49.3050	59.5188	62.6780	64.2371	70.4237	85.4780
	Fares et al. [37]	LW-FSDT	49.2813	59.2366	62.4537	64.4322	70.5642	86.6801
	Pradyumna and Bandyopadhyay [78]	Q9-HSDT	48.7185	58.5305	61.5835	63.1381	69.8604	86.5452
1	Present	SQ8-IFSDT	43.8515	52.9399	55.7458	57.1421	62.8228	76.8258
	Neves et al. [21]	HSDT	43.9548	52.8776	55.6437	57.0255	62.7088	76.6386
	Fares et al. [37]	LW-FSDT	43.8218	52.7402	55.3350	58.2602	62.8351	78.7569
	Pradyumna and Bandyopadhyay [78]	Q9-HSDT	43.4243	52.0173	54.7015	56.0880	62.2152	77.0774

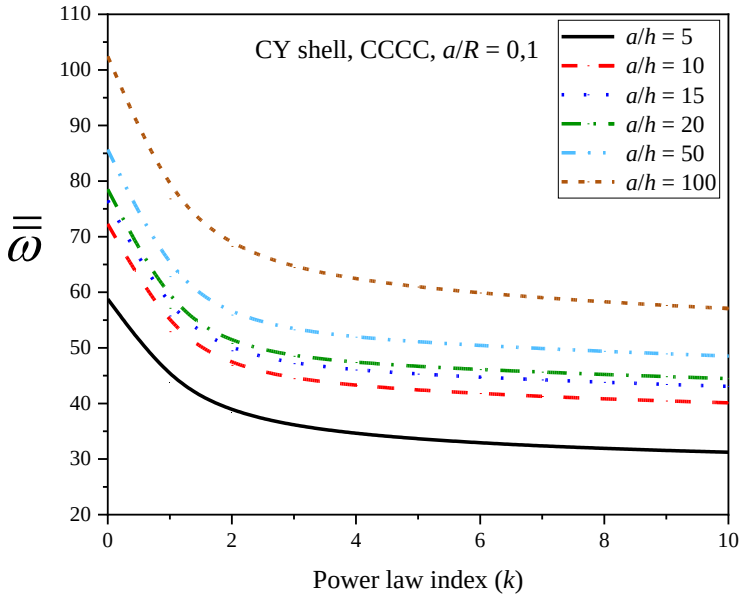

Fig. 8 Effect of side-to-thickness ratios (a/h) on the dimensionless frequencies of CCCC FG (Al/Al_2O_3) cylindrical shells with various power-law factor (k), (a/R = 0.1).

5. Conclusion

An advanced finite element shell model has been developed, effectively employing the IFSDT for analyzing the vibration behavior of functionally graded doubly curved shallow shells. This model excels over traditional models by incorporating a parabolic distribution of transverse shear stress across the thickness, thereby eliminating the conventional requirement for a shear correction factor. Comparisons with established models in existing literature have verified the enhanced reliability and accuracy of the proposed model, confirming its efficacy for exploring the free vibration characteristics of these complex structures. Key contributions and findings of this study include:

- The application of an advanced IFSDT in the new finite element model represents a significant enhancement over traditional approaches. It addresses and overcomes limitations by accurately simulating the transverse shear stress distribution, a crucial factor in the vibration analysis of functionally graded materials.
- A comprehensive parameter analysis highlighted the profound influence of boundary conditions, material gradient index, and the radius-to-length ratio on the vibration behaviors. This study is among the first to quantify these effects, offering a detailed insight that is not extensively covered in existing literature.
- The findings provide actionable insights for the design and manufacture of doubly curved shell structures. The versatility of the developed finite element model extends its utility to complex analyses, making it a valuable tool for future structural designs involving functionally graded materials.

The contributions of this research provide a robust framework for further advancements in the analysis and design of complex shell structures. The novel insights derived from this study contribute significantly to the existing body of knowledge by clarifying the effects of key structural and material parameters on the performance of functionally graded doubly curved shells.

References

1. Garg, A., Mukhopadhyay, T., Belarbi, M. O., & Li, L. Random forest-based surrogates for transforming the behavioral predictions of laminated composite plates and shells from FSDT to Elasticity solutions. Composite Structures, 2023. 309, 116756. https://doi.org/10.1016/j.compstruct.2023.116756
2. Belarbi, M.-O., S.J. Salami, A. Garg, A.-A. Daikh, M.-S.-A. Houari, R. Dimitri, and F. Tornabene, Mechanical behavior analysis of FG-CNT-reinforced polymer composite beams via a hyperbolic shear deformation theory. Continuum Mechanics and Thermodynamics, 2023. **35**(2): p. 497-520. DOI: 10.1007/s00161-023-01191-2.
3. Garg, A., M.-O. Belarbi, H.D. Chalak, and A. Chakrabarti, A review of the analysis of sandwich FGM structures. Composite Structures, 2021. **258**: p. 113427. DOI: https://doi.org/10.1016/j.compstruct.2020.113427.

4. Hirane, H., M.-O. Belarbi, M.S.A. Houari, and A. Tounsi, On the layerwise finite element formulation for static and free vibration analysis of functionally graded sandwich plates. Engineering with Computers, 2022. **38**(5): p. 3871-3899. DOI: 10.1007/s00366-020-01250-1.

5. Sah, S.K. and Ghosh, A., Influence of porosity distribution on free vibration and buckling analysis of multi-directional functionally graded sandwich plates. Composite Structures, 2022. **279**: p. 114795. DOI: https://doi.org/10.1016/j.compstruct.2021.114795.

6. Phung-Van, P., Thai, C.H., Ferreira, A.J.M., and Rabczuk, T., Isogeometric nonlinear transient analysis of porous FGM plates subjected to hygro-thermo-mechanical loads. Thin-Walled Structures, 2020. **148**: p. 106497. DOI: https://doi.org/10.1016/j.tws.2019.106497.

7. Su, J., He, W., and Zhou, K., Study on vibration behavior of functionally graded porous material plates immersed in liquid with general boundary conditions. Thin-Walled Structures, 2023. **182**: p.110166. DOI: https://doi.org/10.1016/j.tws.2022.110166.

8. Zanussi, V.P, Shahverdi, H., Khalafi, V., and Navardi, M.M., Nonlinear flutter analysis of arbitrary functionally graded plates using Isogeometric approach. Thin-Walled Structures, 2023. **182**: p. 110236. DOI: https://doi.org/10.1016/j.tws.2022.110236.

9. Van Vinh, P. Chinh, N.V., and Tounsi, A., Static bending and buckling analysis of bi-directional functionally graded porous plates using an improved first-order shear deformation theory and FEM. European Journal of Mechanics – A/Solids, 2022. **96**: p. 104743. DOI: https://doi.org/10.1016/j.euromechsol.2022.104743.

10. Van Vinh, P., M.-O. Belarbi, M. Avcar, and Ö. Civalek, An improved first-order mixed plate element for static bending and free vibration analysis of functionally graded sandwich plates. Archive of Applied Mechanics, 2023. **93**(5): p. 1841-1862. DOI: 10.1007/s00419-022-02359-z.

11. Punera, D. and T. Kant, A critical review of stress and vibration analyses of functionally graded shell structures. Composite Structures, 2019. **210**: p. 787-809. DOI: https://doi.org/10.1016/j.compstruct.2018.11.084.

12. Loy, C., K. Lam, and J. Reddy, Vibration of functionally graded cylindrical shells. International Journal of Mechanical Sciences, 1999. **41**(3): p. 309-324.

13. Kim, Y.-W., Temperature dependent vibration analysis of functionally graded rectangular plates. Journal of Sound and Vibration, 2005. **284**(3): p. 531-549. DOI: https://doi.org/10.1016/j.jsv.2004.06.043.

14. Ferreira, A.J.M., R.C. Batra, C.M.C. Roque, L.F. Qian, and R.M.N. Jorge, Natural frequencies of functionally graded plates by a meshless method. Composite Structures, 2006. **75**(1): p. 593-600. DOI: https://doi.org/10.1016/j.compstruct.2006.04.018.

15. Belarbi, M. O., Li, L., Ahmed Houari, M. S., Garg, A., Chalak, H. D., Dimitri, R., & Tornabene, F. Nonlocal vibration of functionally graded nanoplates using a layerwise theory. Mathematics and Mechanics of Solids, 2022. 27(12), 2634-2661. https://doi.org/10.1177/10812865221078571

16. Matsunaga, H.. Free vibration and stability of functionally graded circular cylindrical shells according to a 2D higher-order deformation theory. Composite Structures, 2009, 88(4), 519-531.

17. Zhao, X., Y.Y. Lee, and K.M. Liew, Free vibration analysis of functionally graded plates using the element-free kp-Ritz method. Journal of Sound and Vibration, 2009. **319**(3): p. 918-939. DOI: https://doi.org/10.1016/j.jsv.2008.06.025.

18. Pradyumna, S. and J. Bandyopadhyay, Free vibration and buckling of functionally graded shell panels in thermal environments. International Journal of Structural Stability and Dynamics, 2010. **10**(05): p. 1031-1053.

19. Malekzadeh, P. and A. Alibeygi Beni, Free vibration of functionally graded arbitrary straight-sided quadrilateral plates in thermal environment. Composite Structures, 2010. **92**(11): p. 2758-2767. DOI: https://doi.org/10.1016/j.compstruct.2010.04.011.

20. Talha, M. and B.N. Singh, Static response and free vibration analysis of FGM plates using higher order shear deformation theory. Applied Mathematical Modelling, 2010. **34**(12): p. 3991-4011. DOI: https://doi.org/10.1016/j.apm.2010.03.034.

21. Kiani, Y., M. Shakeri, and M. Eslami, Thermoelastic free vibration and dynamic behaviour of an FGM doubly curved panel via the analytical hybrid Laplace–Fourier transformation. Acta Mechanica, 2012. **223**(6): p. 1199-1218.

22. Kim, Y.-W., Free vibration analysis of FGM cylindrical shell partially resting on Pasternak elastic foundation with an oblique edge. Composites Part B: Engineering, 2015. **70**: p. 263-276. DOI: https://doi.org/10.1016/j.compositesb.2014.11.024.

23. Fallah, A., M. Aghdam, and M. Kargarnovin, Free vibration analysis of moderately thick functionally graded plates on elastic foundation using the extended Kantorovich method. Archive of Applied Mechanics, 2013. **83**: p. 177-191.

24. Natarajan, S. and G. Manickam, Bending and vibration of functionally graded material sandwich plates using an accurate theory. Finite Elements in Analysis and Design, 2012. **57**: p. 32-42. DOI: https://doi.org/10.1016/j.finel.2012.03.006.

25. Viola, E., L. Rossetti, and N. Fantuzzi, Numerical investigation of functionally graded cylindrical shells and panels using the generalized unconstrained third order theory coupled with the stress recovery. Composite Structures, 2012. **94**(12): p. 3736-3758. DOI: https://doi.org/10.1016/j.compstruct.2012.05.034.

26. Neves, A.M.A., A.J.M. Ferreira, E. Carrera, M. Cinefra, C.M.C. Roque, R.M.N. Jorge, and C.M.M. Soares, Free vibration analysis of functionally graded shells by a higher-order shear deformation theory and radial basis functions collocation, accounting for through-the-thickness deformations. European Journal of Mechanics - A/Solids, 2013. **37**: p. 24-34. DOI: https://doi.org/10.1016/j.euromechsol.2012.05.005.

27. Jha, D.K., T. Kant, K. Srinivas, and R.K. Singh, An accurate higher order displacement model with shear and normal deformations effects for functionally graded plates. Fusion Engineering and Design, 2013. **88**(12): p. 3199-3204. DOI: https://doi.org/10.1016/j.fusengdes.2013.10.002.

28. Kar, V.R. and S.K. Panda. Free vibration responses of functionally graded spherical shell panels using finite element method. in Gas Turbine India Conference. 2013. American Society of Mechanical Engineers.

29. Tornabene, F., N. Fantuzzi, and M. Bacciocchi, Free vibrations of free-form doubly-curved shells made of functionally graded materials using higher-order equivalent single layer theories. Composites Part B: Engineering, 2014. **67**: p. 490-509.

30. Huy Bich, D., N. Dinh Duc, and T. Quoc Quan, Nonlinear vibration of imperfect eccentrically stiffened functionally graded double curved shallow shells resting on elastic foundation using the first order shear deformation theory. International Journal of Mechanical Sciences, 2014. **80**: p. 16-28. DOI: https://doi.org/10.1016/j.ijmecsci.2013.12.009.

31. Bahadori, R. and M.M. Najafizadeh, Free vibration analysis of two-dimensional functionally graded axisymmetric cylindrical shell on Winkler–Pasternak elastic foundation by First-order Shear Deformation Theory and using Navier-differential quadrature solution methods. Applied Mathematical Modelling, 2015. **39**(16): p. 4877-4894. DOI: https://doi.org/10.1016/j.apm.2015.04.012.

32. Nguyen, T.N., C.H. Thai, and H. Nguyen-Xuan, A novel computational approach for functionally graded isotropic and sandwich plate structures based on a rotation-free meshfree method. Thin-Walled Structures, 2016. **107**: p. 473-488. DOI: https://doi.org/10.1016/j.tws.2016.06.011.

33. Fantuzzi, N., S. Brischetto, F. Tornabene, and E. Viola, 2D and 3D shell models for the free vibration investigation of functionally graded cylindrical and spherical panels. Composite Structures, 2016. **154**: p. 573-590. DOI: https://doi.org/10.1016/j.compstruct.2016.07.076.

34. Wang, Y. and D. Wu, Free vibration of functionally graded porous cylindrical shell using a sinusoidal shear deformation theory. Aerospace Science and Technology, 2017. **66**: p. 83-91.

35. Kant, T. and D. Punera. A refined higher order theory for statics and dynamics of doubly curved shells. in Proc Indian Natl Sci Acad. 2017.

36. Shi, D., S. Zha, H. Zhang, and Q. Wang, Free Vibration Analysis of the Unified Functionally Graded Shallow Shell with General Boundary Conditions. Shock and Vibration, 2017. **2017**: p. 7025190. DOI: 10.1155/2017/7025190.

37. Punera, D. and T. Kant, Free vibration of functionally graded open cylindrical shells based on several refined higher order displacement models. Thin-Walled Structures, 2017. **119**: p. 707-726.

38. Parand, A.A. and A. Alibeigloo, Static and vibration analysis of sandwich cylindrical shell with functionally graded core and viscoelastic interface using DQM. Composites Part B: Engineering, 2017. **126**: p. 1-16.

39. Khayat, M., S.M. Dehghan, M.A. Najafgholipour, and A. Baghlani, Free vibration analysis of functionally graded cylindrical shells with different shell theories using semi-analytical method. Steel and Composite Structures, An International Journal, 2018. **28**(6): p. 735-748.

40. Pandey, S. and S. Pradyumna, Analysis of functionally graded sandwich plates using a higher-order layerwise theory. Composites Part B: Engineering, 2018. **153**: p. 325-336. DOI: https://doi.org/10.1016/j.compositesb.2018.08.121.

41. Li, H., F. Pang, H. Chen, and Y. Du, Vibration analysis of functionally graded porous cylindrical shell with arbitrary boundary restraints by using a semi analytical method. Composites Part B: Engineering, 2019. **164**: p. 249-264.

42. Fares, M.E., M.K. Elmarghany, D. Atta, and M.G. Salem, Bending and free vibration of multilayered functionally graded doubly curved shells by an improved layerwise theory. Composites Part B: Engineering, 2018. **154**: p. 272-284. DOI: https://doi.org/10.1016/j.compositesb.2018.07.038.

43. Sofiyev, A.H. and D. Hui, On the vibration and stability of FGM cylindrical shells under external pressures with mixed boundary conditions by using FOSDT. Thin-Walled Structures, 2019. **134**: p. 419-427. DOI: https://doi.org/10.1016/j.tws.2018.10.018.

44. Sofiyev, A.H., D. Hui, V.C. Haciyev, H. Erdem, G.Q. Yuan, E. Schnack, and V. Guldal, The nonlinear vibration of orthotropic functionally graded cylindrical shells surrounded by an elastic foundation within first order shear deformation theory. Composites Part B: Engineering, 2017. **116**: p. 170-185. DOI: https://doi.org/10.1016/j.compositesb.2017.02.006.

45. Shi, D., S. Zha, H. Zhang, and Q. Wang, Free vibration analysis of the unified functionally graded shallow shell with general boundary conditions. Shock and Vibration, 2017. **2017**.

46. Zare Jouneghani, F., R. Dimitri, M. Bacciocchi, and F. Tornabene, Free Vibration Analysis of Functionally Graded Porous Doubly-Curved Shells Based on the First-Order Shear Deformation Theory. Applied Sciences, 2017. **7**(12): p. 1252.

47. Pang, F., H. Li, F. Jing, and Y. Du, Application of First-Order Shear Deformation Theory on Vibration Analysis of Stepped Functionally Graded Paraboloidal Shell with General Edge Constraints. Materials, 2019. **12**(1): p. 69.

48. Li, H., F. Pang, Y. Ren, X. Miao, and K. Ye, Free vibration characteristics of functionally graded porous spherical shell with general boundary conditions by using first-order shear deformation theory. Thin-Walled Structures, 2019. **144**: p. 106331.

49. Li, H., F. Pang, Y. Li, and C. Gao, Application of first-order shear deformation theory for the vibration analysis of functionally graded doubly-curved shells of revolution. Composite Structures, 2019. **212**: p. 22-42.

50. Tran, M.-T., V.-L. Nguyen, S.-D. Pham, and J. Rungamornrat, Free vibration of stiffened functionally graded circular cylindrical shell resting on Winkler–Pasternak foundation with different boundary conditions under thermal environment. Acta mechanica, 2020. **231**: p. 2545-2564.

51. Van Long, N., T.I. Thinh, D.H. Bich, and T.M. Tu, Nonlinear dynamic responses of sandwich-FGM doubly curved shallow shells subjected to underwater explosions using first-order shear deformation theory. Ocean Engineering, 2022. **260**: p. 111886.

52. Daikh, A.A., Temperature dependent vibration analysis of functionally graded sandwich plates resting on Winkler/Pasternak/Kerr foundation. Materials Research Express, 2019. **6**(6): p. 065702.

53. Arefi, M. and K.K. Żur, Free vibration analysis of functionally graded cylindrical nanoshells resting on Pasternak foundation based on two-dimensional analysis. Steel and Composite Structures, An International Journal, 2020. **34**(4): p. 615-623.

54. Kushnir, R.M., U.V. Zhydyk, and V.M. Flyachok, Thermoelastic Analysis of Functionally Graded Cylindrical Shells. Journal of Mathematical Sciences, 2021. **254**(1): p. 46-58. DOI: 10.1007/s10958-021-05287-5.

55. Sayyad, A.S. and Y.M. Ghugal, Static and free vibration analysis of doubly-curved functionally graded material shells. Composite Structures, 2021. **269**: p. 114045.

56. Pham, Q.-H., T.T. Tran, V.K. Tran, P.-C. Nguyen, T. Nguyen-Thoi, and A.M. Zenkour, Bending and hygro-thermo-mechanical vibration analysis of a functionally graded porous sandwich nanoshell resting on elastic foundation. Mechanics of Advanced Materials and Structures, 2022. **29**(27): p. 5885-5905.

57. Shinde, B.M. and A.S. Sayyad, A new higher order shear and normal deformation theory for FGM sandwich shells. Composite Structures, 2022. **280**: p. 114865.

58. Van Vinh, P., A. Tounsi, and M.-O. Belarbi, On the nonlocal free vibration analysis of functionally graded porous doubly curved shallow nanoshells with variable nonlocal parameters. Engineering with Computers, 2023. **39**(1): p. 835-855. DOI: 10.1007/s00366-022-01687-6.

59. Belarbi, M.-O., A.A. Daikh, A. Garg, H. Hirane, M.S.A. Houari, Ö. Civalek, and H. Chalak, Bending and free vibration analysis of porous functionally graded sandwich plate with various porosity distributions using an extended layerwise theory. Archives of Civil and Mechanical Engineering, 2022. **23**(1): p. 15.

60. Hu, Z., C. Zhou, X. Zheng, Z. Ni, and R. Li, Free vibration of non-Lévy-type functionally graded doubly curved shallow shells: New analytic solutions. Composite Structures, 2023. **304**: p. 116389.

61. Nguyen, V.D., Static bending, free vibration, and buckling analyses of two-layer FGM plates with shear connectors resting on elastic foundations. Alexandria Engineering Journal, 2023. **62**: p. 369-390.

62. Sofiyev, A. and N. Fantuzzi, Analytical solution of stability and vibration problem of clamped cylindrical shells containing functionally graded layers within shear deformation theory. Alexandria Engineering Journal, 2023. **64**: p. 141-154.

63. Sayyad, A.S., Y.M. Ghugal, and T. Kant, Higher-order static and free vibration analysis of doubly-curved FGM sandwich shallow shells. Forces in Mechanics, 2023. **11**: p. 100194. DOI: https://doi.org/10.1016/j.finmec.2023.100194.

64. Ghandourah, E.E., A.A. Daikh, S. Khatir, A.M. Alhawsawi, E.M. Banoqitah, and M.A. Eltaher, A Dynamic Analysis of Porous Coated Functionally Graded Nanoshells Rested on Viscoelastic Medium. Mathematics, 2023. **11**(10): p. 2407.

65. Mouthanna, A., S.H. Bakhy, M. Al-Waily, and E.K. Njim, Free Vibration Investigation of Single-Phase Porous FG Sandwich Cylindrical Shells: Analytical, Numerical and Experimental Study. Iranian Journal of Science and Technology, Transactions of Mechanical Engineering, 2023. DOI: 10.1007/s40997-023-00700-7.

66. Daikh, A.-A., M.-O. Belarbi, D. Ahmed, M.S.A. Houari, M. Avcar, A. Tounsi, and M.A. Eltaher, Static analysis of functionally graded plate structures resting on variable elastic foundation under various boundary conditions. Acta Mechanica, 2023. **234**(2): p. 775-806. DOI: 10.1007/s00707-022-03405-1.

67. Armendáriz Hernández, M.T., A. Díaz Díaz, C.H. Rubio Rascón, and R. Castañeda Balderas, A new finite element for the analysis of functionally graded shells. Thin-Walled Structures, 2023. **186**: p. 110659. DOI: https://doi.org/10.1016/j.tws.2023.110659.

68. Deepak, P., K. Jayakumar, and S. Panda, Functionally graded doubly-curved shell with temperature dependent material properties and surface-mounted MEE layers. Mechanics of Advanced Materials and Structures: p. 1-16. DOI: 10.1080/15376494.2023.2285409.

69. Rachid, A., D. Ouinas, A. Lousdad, F.Z. Zaoui, B. Achour, H. Gasmi, T.A. Butt, and A. Tounsi, Mechanical behavior and free vibration analysis of FG doubly curved shells on elastic foundation via a new modified displacements field model of 2D and quasi-3D HSDTs. Thin-Walled Structures, 2022. **172**: p. 108783.

70. Pham, Q.H., T.-A. Nguyen, N.-T. Do, V.K. Tran, and M.-N. Nguyen, Static and vibration analyses of functionally graded porous shell structures by using an averaged edge/node-based smoothed MITC3 element. Computers & Mathematics with Applications, 2024. **153**: p. 56-70. DOI: https://doi.org/10.1016/j.camwa.2023.10.037.

71. Matsunaga, H., Free vibration and stability of functionally graded plates according to a 2-D higher-order deformation theory. Composite Structures, 2008. **82**(4): p. 499-512. DOI: https://doi.org/10.1016/j.compstruct.2007.01.030.

72. Trinh, M.-C. and S.-E. Kim, A three variable refined shear deformation theory for porous functionally graded doubly curved shell analysis. Aerospace Science and Technology, 2019. **94**: p. 105356. DOI: https://doi.org/10.1016/j.ast.2019.105356.

73. Alijani, F., M. Amabili, K. Karagiozis, and F. Bakhtiari-Nejad, Nonlinear vibrations of functionally graded doubly curved shallow shells. Journal of Sound and Vibration, 2011. **330**(7): p. 1432-1454. DOI: https://doi.org/10.1016/j.jsv.2010.10.003.

74. Chorfi, S.M. and A. Houmat, Non-linear free vibration of a functionally graded doubly-curved shallow shell of elliptical plan-form. Composite Structures, 2010. **92**(10): p. 2573-2581. DOI: https://doi.org/10.1016/j.compstruct.2010.02.001.

75. Van Vinh, P. and A. Tounsi, Free vibration analysis of functionally graded doubly curved nanoshells using nonlocal first-order shear deformation theory with variable nonlocal parameters. Thin-Walled Structures, 2022. **174**: p. 109084. DOI: https://doi.org/10.1016/j.tws.2022.109084.

76. Pradyumna, S. and J.N. Bandyopadhyay, Free vibration and buckling of functionally graded shell panels in thermal environments. International Journal of Structural Stability and Dynamics, 2010. **10**(05): p. 1031-1053. DOI: 10.1142/s0219455410003889.

77. Zhao, X., Y.Y. Lee, and K.M. Liew, Thermoelastic and vibration analysis of functionally graded cylindrical shells. International Journal of Mechanical Sciences, 2009. **51**(9): p. 694-707. DOI: https://doi.org/10.1016/j.ijmecsci.2009.08.001.

78. Pradyumna, S. and J.N. Bandyopadhyay, Free vibration analysis of functionally graded curved panels using a higher-order finite element formulation. Journal of Sound and Vibration, 2008. **318**(1): p. 176-192. DOI: https://doi.org/10.1016/j.jsv.2008.03.056.